Available online at www.sciencedirect.com
SCIENCE DIRECT®
Journal of Sound and Vibration 281 (2005) 647–673
JOURNAL OF SOUND AND VIBRATION
www.elsevier.com/locate/jsvi

Buffeting response of long-span cable-supported bridges under skew winds. Part 1: theory

L.D. Zhu[a,*], Y.L. Xu[b]

[a]*State Key Laboratory for Disaster Reduction in Civil Engineering, Department of Bridge Engineering, Tongji University, 1239 Siping Road, Shanghai 200092, China*
[b]*Department of Civil and Structural Engineering, The Hong Kong Polytechnic University, Hung Hom, Kowloon, Hong Kong, China*

Received 4 April 2003; received in revised form 20 January 2004; accepted 29 January 2004
Available online 23 September 2004

Abstract

A finite-element-based framework for buffeting analysis of long-span cable-supported bridges under skew winds is developed in the frequency domain utilizing the linear quasi-steady theory and the strip theory of aerodynamics in conjunction with the pseudo excitation method. A set of universal expressions for six components of buffeting forces is first derived in association with oblique cross-sections of bridge components, in which the buffeting forces are formed with respect to the wind coordinate system and then converted to those with respect to the structural coordinate system. Skew mean wind and three orthogonal components of velocity fluctuations can thus be easily handled without any further decomposition. The coherence between velocity fluctuations of wind turbulence at any two arbitrary spatial points is considered in the global wind coordinate system rather than in the global structural coordinate system. Aeroelastic stiffness and damping matrices due to self-excited forces are then taken into consideration in terms of the 18 flutter derivatives with respect to the oblique cross-sections. The pseudo-excitation method is finally employed to solve efficiently the fully coupled 3D buffeting problem of long-span cable-supported bridges under skew winds with the effects of multi-modes and spatial modes, inter-mode coupling and aerodynamic coupling, and the interaction among major bridge components being naturally included.

*Corresponding author. Tel.: +86-21-65983116X2309; fax: 86-21-65984882.
E-mail address: ledong@mail.tongji.edu.cn (L.D. Zhu).

0022-460X/$ - see front matter © 2004 Elsevier Ltd. All rights reserved.
doi:10.1016/j.jsv.2004.01.026

Nomenclature

a subscript representing one of the turbulence components, u, v, w

$\mathbf{a}$ $3m$-dimensional vector of turbulence components of entire bridge

$\bar{\mathbf{a}}$ 3D vector of turbulence components of a segment

$\bar{\mathbf{A}}^b$ 6×3 aerodynamic coefficient matrix of buffeting forces per unit length with respect to $\bar{q}\bar{p}\bar{h}$-system due to fluctuating winds

A_i^* flutter derivatives for self-excited pitching moment on bridge deck due to deck motion

B characteristic width of bridge component

$\mathbf{B}$ $\mathbf{Diag}(B, B, B, B^2, B^2, B^2)$

$\tilde{\mathbf{C}}$ 6D vector of rms aerodynamic coefficients at $\tilde{\beta}$ and $\tilde{\theta}$

$\bar{\mathbf{C}}$ 6D vector of aerodynamic coefficient at $\bar{\beta}$ and $\bar{\theta}$

$\mathbf{C}^s$ $6N \times 6N$ structural damping matrix of bridge

$\tilde{\mathbf{C}}^s$ $M_\Phi \times M_\Phi$ generalized structural damping matrix of bridge

$\mathbf{C}^{\mathrm{se}}$ $6N \times 6N$ aerodynamic damping matrix of bridge

$\tilde{\mathbf{C}}^{\mathrm{se}}$ $M_\Phi \times M_\Phi$ generalized aerodynamic damping matrix of bridge

$C_{C_{\bar{q}}}$ aerodynamic coefficient of crosswind force along axis $\bar{q}$

$C_{D_{\bar{p}}}$ aerodynamic coefficient of drag along axis $\bar{p}$

$C_{L_{\bar{h}}}$ aerodynamic coefficient of lift along axis $\bar{h}$

$C_{M_{\tilde{\alpha}}}$ aerodynamic coefficient of pitching moment around axis $\bar{q}$

$C_{M_{\tilde{\gamma}}}$ aerodynamic coefficient of rolling moment around axis $\bar{p}$

$C_{M_{\tilde{\phi}}}$ aerodynamic coefficient of yawing moment around axis $\bar{h}$

$C_{\bar{q}}^b$ buffeting crosswind force per unit length along axis $\bar{q}$

$C_{X_u}^a$ turbulence coherence decay coefficient of component a in X_u direction

$C_{Y_v}^a$ turbulence coherence decay coefficient of component a in Y_v direction

$C_{Z_w}^a$ turbulence coherence decay coefficient of component a in Z_w direction

$\mathbf{d}$ $3m \times 3m$ real diagonal matrix of $\mathbf{l}^*\mathbf{d}\mathbf{l}^{\mathrm{T}}$ decomposition of $\mathbf{S}_{aa}$

d_j jth nonzero diagonal element of matrix $\mathbf{d}$

$\mathbf{D}$ $M_\Phi \times M_\Phi$ diagonal matrix of $\mathbf{L}^*\mathbf{D}\mathbf{L}^{\mathrm{T}}$ decomposition of $\mathbf{S}_{\tilde{\mathrm{F}}\tilde{\mathrm{F}}}^b$

$\mathbf{Diag}$ diagonal matrix

$D_{\bar{p}}^b$ buffeting drag per unit length along axis $\bar{p}$

D_p^{se} self-excited drag per unit length along axis p

D_r rth nonzero diagonal element of matrix $\mathbf{D}$

$\mathbf{F}^b$ $6N$-dimensional vector of buffeting forces in XYZ-system

$\tilde{\mathbf{F}}^b$ M_Φ-dimensional vector of generalized buffeting forces

$\mathbf{F}^{\mathrm{se}}$ $6N$-dimensional vector of aeroelastic forces in XYZ-system

$\mathbf{F}_{e,k}^b$ 12D vector of nodal buffeting forces of kth element in XYZ- system

$\tilde{\mathbf{f}}^{\mathrm{ad}}$ 6D vector of total wind forces per unit length in $\tilde{q}\tilde{p}\tilde{h}$-system

$\bar{\mathbf{f}}^b$ 6D vector of buffeting forces per unit length in $\bar{q}\bar{p}\bar{h}$-system

$\mathbf{f}_{e,k}^b$ 12D nodal buffeting force vector of kth element in xyz-system

G_S used as a subscript, representing the global structural XYZ-system

G_W used as a subscript, representing the global wind $X_uY_vZ_w$-system

$\tilde{\mathbf{H}}$ $M_\Phi \times M_\Phi$ matrix of generalized frequency response function

H_i^* flutter derivative for deck self-excited lift

K reduced frequency

$\tilde{\mathbf{K}}$ $M_\Phi \times M_\Phi$ matrix of total generalized stiffness of bridge

$\mathbf{K}^s$ $6N \times 6N$ structural stiffness matrix of bridge

$\tilde{\mathbf{K}}^s$ $M_\Phi \times M_\Phi$ generalized structural stiffness matrix of bridge

$\mathbf{K}^{se}$ $6N \times 6N$ aerodynamic stiffness matrix of bridge

$\tilde{\mathbf{K}}^{se}$ $M_\Phi \times M_\Phi$ generalized aerodynamic stiffness matrix of bridge

$\mathbf{l}$ $3m \times 3m$ lower triangular complex matrix of $\mathbf{l}^*\mathbf{d}\mathbf{l}^T$ decomposition of $\mathbf{S}_{aa}$

$\mathbf{l}_j$ jth column of lower triangular complex matrix $\mathbf{l}$

$\mathbf{L}$ $M_\Phi \times M_\Phi$ lower triangular matrix of $\mathbf{L}^*\mathbf{D}\mathbf{L}^T$ decomposition $\mathbf{S}^b_{\tilde{F}\tilde{F}}$

$L_a^{x_u}$ length scale of turbulence component a in the alongwind direction

L_h^{se} aeroelastic lift per unit length along axis h

$L_{\bar{h}}^b$ buffeting lift per unit length along axis $\bar{h}$

$L_{i,k}$ length of ith segment of kth element

L_k length of kth element

$\mathbf{L}_r$ rth column of lower triangular complex matrix $\mathbf{L}$

L_r used as a subscript, representing the local reference coordinate qph-system

L_s used as a subscript, representing the local structural coordinate xyz-system

$L_{\bar{w}}$ used as a subscript, representing the local mean wind $\bar{q}\bar{p}\bar{h}$-system

$L_{\tilde{w}}$ used as a subscript, representing the local instantaneous wind $\tilde{q}\tilde{p}\tilde{h}$-system

m total number of segments in bridge FE model

M number of elements of bridge FE model

$\tilde{\mathbf{M}}^s$ $M_\Phi \times M_\Phi$ generalized mass matrix of structure

M_Φ number of modes used in buffeting analysis

M_α^{se} self-excited pitching moment per unit length around axis q

$M_{\bar{\alpha}}^b$ buffeting pitching moment per unit length around axis $\bar{q}$

$M_{\bar{\gamma}}^b$ buffeting rolling moment per unit length around axis $\bar{p}$

$M_{\bar{\phi}}^b$ buffeting yawing moment per unit length around axis $\bar{h}$

n frequency of turbulence

n_k total number of segments of kth element

n_{xa} modified turbulence frequency with turbulence scale effect

N total number of nodes of the bridge FE model

$\mathbf{N}_{\delta,k}$ 6×12 displacement interpolation matrix of kth element in xyz-system

$\mathbf{P}^b$ $6N \times 3m$ coefficient matrix of nodal buffeting forces

P_i^* flutter derivatives for self-excited drag on bridge deck

$\mathbf{P}^b_{i,k}$ 12×3 coefficient matrix of nodal buffeting forces of kth element in XYZ-system due to wind turbulence on the ith segment

qph local reference coordinate system of an element,

$\bar{q}\bar{p}\bar{h}$ local mean wind coordinate system of an element

$\tilde{q}\tilde{p}\tilde{h}$ local instantaneous wind coordinate system of an element

$R_{a_{1_{P_1}} a_{2_{P_2}}}$ root-coherence function between the turbulence components a_1 at point P_1 and a_2 at point P_2

$\mathbf{S}_{aa}$ $3m \times 3m$ spectral matrix of wind turbulence on the entire bridge

$\mathbf{S}^b_{FF}$ $6N \times 6N$ spectral matrix of nodal buffeting force $\mathbf{F}^b$ of the entire bridge

$\mathbf{S}^b_{\tilde{F}\tilde{F}}$ $M_\Phi \times M_\Phi$ spectral matrix of generalized buffeting force $\tilde{\mathbf{F}}^b$

$\mathbf{S}_{\bar{a}_{i,k}\bar{a}_{j,l}}$ 3×3 spectral matrix between one of the turbulence components at the ith segment center of the kth element and one of those at the jth segment center of the lth element

$S_{a_{1_{P_1}} a_{2_{P_2}}}$ spectrum between the turbulence component a_1 at point P_1 and the turbulence component a_2 at point P_2

$S_{a_{i,k}a_{j,l}}$ spectrum between a turbulence component at the ith segment center of the kth element and a turbulence

	component at the jth segment center of the lth element
$\mathbf{S}_{\Delta_i}$	auto-spectral vector of displacement responses at ith node
$\mathbf{S}_{\Delta\Delta}$	$6N \times 6N$ response spectral matrix of bridge nodal displacements
$\mathbf{S}_{\eta\eta}$	$M_\Phi \times M_\Phi$ response spectral matrix of generalized displacements
$\mathbf{T}_{S_1S_2}$	3×3 transformation matrix from the coordinate system S_2 to the coordinate system S_1 (S_1 and S_2 ($S_1 \neq S_2$) can be any two of G_W, G_S, L_s, L_r, $L_{\bar{w}}$ and $L_{\tilde{w}}$)
$\bar{\mathbf{T}}_{S_1S_2}$	$\mathbf{Diag}(\mathbf{T}_{S_1S_2}, \mathbf{T}_{S_1S_2})$
$\hat{\mathbf{T}}_{S_1S_2}$	$\mathbf{Diag}(\mathbf{T}_{S_1S_2}, \mathbf{T}_{S_1S_2}, \mathbf{T}_{S_1S_2}, \mathbf{T}_{S_1S_2})$
t_{ij}	the element of the ith row and jth column of the 3×3 matrix $\mathbf{T}_{LrGw}$
$\bar{U}$	mean wind speed
u	fluctuating wind speed along mean wind
v	lateral fluctuating wind speed in horizontal direction
V	instantaneous wind speed
w	upward fluctuating wind speed
xyz	local structural coordinate system of an element
XYZ	global structural coordinate system
$X_uY_vZ_w$	global wind coordinate system
β_0	global yaw angle of mean wind relative to bridge
$\bar{\beta}$	local yaw angle of mean wind relative to an element
$\tilde{\beta}$	local yaw angle of instantaneous wind relative to an element
$\chi_{\tilde{f}a}$	aerodynamic admittance functions between the buffeting force $\tilde{f}$ and turbulence component a ($\tilde{f} = C_{\tilde{q}}, D_{\tilde{p}}, L_{\tilde{h}}, M_{\tilde{\alpha}}, M_{\tilde{\gamma}}, M_{\tilde{\phi}}$; $a = u, v, w$)
$\mathbf{\Delta}$	$6N$-dimensional vector of bridge nodal displacements in XYZ-system
$\mathbf{\Delta}_i$	6D vector of displacement response at ith node
$\Delta\beta$	increment of local wind yaw due to fluctuating wind speed
$\Delta\theta$	increment of local wind inclination due to fluctuating wind speed
δ_h	dynamic translational displacement of an element section along axis h
δ_p	dynamic translational displacement of an element section along axis p
δ_α	dynamic angular displacement of an element section around axis q
$\mathbf{\Phi}$	$6N \times M_\Phi$ mode shape matrix of bridge
Γ	gamma function
η	M_Φ-dimensional vector of generalized displacement coordinates
$\eta_{p,r}$	rth harmonic generalized pseudo-displacement response vector
$\boldsymbol{\phi}_r$	rth mode shape vector of bridge
θ_0	global inclination of mean wind relative to bridge
$\bar{\theta}$	local inclination of mean wind relative to an element
$\tilde{\theta}$	local inclination of instantaneous wind relative to an element
ρ	air density
$\boldsymbol{\sigma}_{\Delta_i}$	6D vector of displacement response at ith node
ω	circular frequency of structural vibration or wind turbulence
ω_r	rth modal circular frequency of bridge in static air
ξ	reduced coordinate of element
ζ_r	rth modal damping ratio of bridge in static air
$()'^{\beta}$	$\partial()/\partial\beta$, partial derivatives with respect to local yaw angle
$()'^{\theta}$	$\partial()/\partial\theta$, partial derivatives with respect to local inclination angle

1. Introduction

With increasing span length, modern long-span cable-supported bridges become more and more flexible and susceptible to strong winds. This leads to a significant increase of buffeting

response of the bridges, which in turn may result in a substantial increase in stresses or serious fatigue damage to structural components and connections. Therefore, an accurate prediction of buffeting response of long-span cable-supported bridges due to strong winds becomes more and more important.

Most of the existing buffeting analysis methods are based on the aerodynamic strip theory and the quasi-steady linear theory, such as those developed by Davenport [1–3], Scanlan and Gade [4], Scanlan [5] and Lin [6,7], Lin and Yang [8]. These methods have been continuously refined by researchers as a result of the enhancement of computer technique and capacity as well as the demand for more accurate prediction of buffeting response of modern long-span bridges. Nowadays, not only the effects of multi-modes, inter-mode coupling, and aerodynamic coupling but also the interaction between major bridge components can be included in either the time domain [9–11] or the frequency domain [12–17]. However, most of the previous investigations take incident mean wind at a right angle to the longitudinal axis of the bridge. This may not always be the case when the bridge is located in a complex and heterogeneous topography and attacked by a typhoon. The recent field measurements on the Tsing Ma Suspension Bridge during typhoons clearly demonstrated that strong winds seldom attacked the bridge in a direction normal to the bridge longitudinal axis [18,19]. Although some efforts have been made to take into consideration skew winds in buffeting analysis of bridges [20–24], they are all based on the decomposition approach (cosine and sine rules). That is, the mean yaw wind is decomposed into two components: one is normal and the other parallel to the bridge span. The contribution of the parallel mean wind component is then either ignored or separately analyzed from that of the normal mean wind component. The difficult and intractable issues associated with the decomposition approach are: (1) how to decompose velocity fluctuations of turbulent wind with respect to the bridge axis, (2) how to calculate practically the buffeting response to the parallel wind component and (3) how to compose the calculated response components. Furthermore, if the parallel wind component is neglected, the buffeting response of a long-span bridge due to yaw wind obtained by taking the decomposition approach would be always smaller than that due to normal wind of the same wind speed. However, some wind tunnel tests revealed that buffeting response due to yaw wind would reach the same level as that due to the normal wind [24–29]. This indicates that the decomposition approach may underestimate the buffeting response of bridges under yaw wind and may not truly reflect the effects of buffeting action due to skew wind on the bridge.

While refining the existing buffeting analysis method, special attention has been paid to the comparison of bridge buffeting response between field measurement results and analytical results [30,31] aiming to verify various assumptions involved in the analytical method. However, it is quite a difficult and challenging task and needs an appropriate analytical method for predicting the buffeting response of the bridge due to skew winds. Furthermore, a rational buffeting analysis of a long-span cable-supported bridge under skew winds is also needed in order to have a better evaluation of probability or risk analysis of the bridge exposed to local wind climate.

In this connection, this paper presents a finite element (FE)-based framework for buffeting analysis of long-span cable-supported bridges under skew winds in the frequency-domain utilizing the linear quasi-steady theory and the oblique strip theory in conjunction with the pseudo-excitation method. The FE framework developed here was applied to the Tsing Ma Suspension Bridge in Hong Kong as a case study. The fundamental aerodynamic information of the bridge

required in the framework, such as the aerodynamic coefficients and flutter derivatives of the bridge deck under skew winds, have been evaluated experimentally by wind tunnel studies and reported in the literatures [32–34]. The computed buffeting response is then compared with the field measured buffeting response of the bridge during Typhoon Sam, and the results from this case study are presented in Part 2 of this paper.

The development of the proposed framework for buffeting analysis under skew winds requires some basic assumptions. Firstly, the incident wind is assumed to be stationary and its mean wind speed $\bar{U}$ is sufficiently larger than any of three fluctuating wind components $u(t)$, $v(t)$, and $w(t)$. Secondly, the mean wind speed used in buffeting analysis falls outside the range that may cause either aeroelastic instability or vortex shedding vibration of the bridge. Thirdly, the average scales of the turbulence are assumed to be sufficiently larger than the chord-wise dimension of the bridge members so that the quasi-steady theory is applicable. Finally, wind-induced bridge vibration is small so that the linear approach can be accepted.

Before presenting the formulation in detail, a general description of the outline of the implementation of the FE framework is necessary and is given as follows:

(1) A global structural coordinate system for the bridge and local structural coordinate systems for the elements are first introduced to establish the FE model of the bridge.
(2) A global wind coordinate system is then presented to describe the mean wind direction by a global yaw angle and inclination of mean wind and the three fluctuating velocity components of wind turbulence.
(3) A local reference coordinate system and a local mean wind coordinate system are introduced for each element to define the local wind direction by a local yaw angle and inclination of mean wind and the buffeting forces on an oblique strip. For the convenient and correct usage of the databases of the measured aerodynamic coefficients and flutter derivatives, the definitions of the two local coordinate systems and the local yaw angle and inclination are in a same manner for all elements, and should be in consistence with those adopted in the corresponding wind tunnel tests. Thus, for an element, its local reference coordinate system may be different from its local structural coordinate system in the FE model because the latter may have different style for different element.
(4) The local yaw angle and inclination of mean wind are determined for every element from the global yaw angle and inclination of mean wind by means of coordinate transformation.
(5) A local instantaneous wind coordinate system is presented for each element to define the aerodynamic forces due to the instantaneous wind, and to determine the increments of the local wind yaw angle and inclination due to the fluctuating wind velocities, which will be used in the Taylor's formula of linearization.
(6) The aerodynamic coefficients and flutter derivatives of all elements are determined from the databases according to the determined local wind yaw angle and inclination.
(7) The model of buffeting forces on an oblique aerodynamic strip due to fluctuating wind velocities is established for each element based on the quasi-steady theory and the Taylor's formula of linearization.
(8) The ensemble vector of buffeting forces on the entire bridge is formed.
(9) The relation between the ensemble spectral matrices of buffeting forces and wind turbulence acting on the entire bridge is established.

(10) The model of self-excited forces on an oblique aerodynamic strip is constituted for each element.
(11) The ensemble vector of self-excited forces on the bridge is formed.
(12) The governing equation of motion of the bridge is established by FE method for buffeting analysis.
(13) The governing equation of motion is finally solved in the frequency domain to obtain the spectral and rms responses, based on the stochastic vibration theory in conjunction with the pseudo-excitation method.

2. Buffeting forces and spectra under skew winds

This section aims to derive the expressions of buffeting forces on a long-span cable-supported bridge under skew winds based on the linear quasi-steady theory and the aerodynamic strip theory. An oblique strip of a bridge component along the mean wind direction is introduced. All the six components of aerodynamic forces acting on the oblique strip due to skew winds, i.e. crosswind, drag and lift forces and pitching, rolling and yawing moments are included. The buffeting forces (moments) are first formed with respect to an element in the wind coordinate system and then transferred to those in the structural coordinate system and finally used to assemble the global buffeting force vector. Clearly, the transformations in this method are carried out on the buffeting forces rather than on the mean and fluctuating winds. This avoids the difficulties involved in the traditional decomposition method [20–24]. The spectral density function matrix of global buffeting forces is then determined with the coherence of wind turbulence between any two arbitrary spatial points being considered in the global wind coordinate system rather than in the global structural coordinate system.

2.1. Coordinate systems and wind direction

Some Cartesian coordinate systems, obeying the right-handed rule, are introduced in this study to facilitate the formulation of buffeting forces. As shown in Fig. 1, XYZ is the global structural coordinate system used to describe the bridge structural model and the overall dynamic equilibrium conditions. $X_uY_vZ_w$ is called the global wind coordinate system, required to define wind direction and fluctuating wind components. The axis X_u is along the direction of mean wind velocity $\bar{U}$ and the axis Y_v is located in a horizontal plane, whilst the axis Z_w is always positive upward. There are many possible combinations between the XYZ-system and the $X_uY_vZ_w$-system in practice. Fig. 1 shows a typical one of these combinations, where, the axis Y_v is parallel to the X–Y plane. The mean wind direction in the global structural coordinate system can then be determined with a global mean wind yaw angle (β_0) in conjunction with a global mean wind inclination angle (θ_0). As shown in Fig. 1, β_0 is defined as the angle between the vertical plane normal to the bridge longitudinal axis and the vertical plane with the mean wind velocity included; θ_0 is interpreted as the angle between the mean wind velocity and the horizontal plane. Furthermore, β_0 is positive when mean wind comes from the right side of the Y–Z plane, and θ_0 is positive when the vertical component of the mean wind velocity is upward.

Fig. 2 shows a typical combination of two local coordinate systems of an arbitrary element (strip), where, *xyz* is called the local structural coordinate system used to present the elemental parameters, such as, the matrices of elemental mass, stiffness, damping and loading, and *qph* is the local reference coordinate system introduced to define the wind direction with respect to the element. The axis q is along the longitudinal axis of the element. The axis p is located in either the deck plane or the tower plane. Its positive direction should be determined in such a way that the angle between the axis p and the mean wind direction is less than 90° and when the mean wind is parallel to the qp plane and normal to the axis q, the axis p is along the mean wind direction.

The local mean wind yaw angle ($\bar{\beta}$) is defined as the angle between the ph-plane and the plane constituted of the mean wind $\bar{U}$ and the axis h. $\bar{\beta}$ is positive when the mean wind component $\bar{U}_q$along the axis q is negative. The local mean wind inclination ($\bar{\theta}$) is defined as the angle between the mean wind velocity and the qp-plane. It takes a positive value when the mean wind component $\bar{U}_h$ along the axis h is positive. Fig. 2 also shows the local yaw angle $\tilde{\beta}$ and inclination angle $\tilde{\theta}$ of instantaneous wind, which determine the direction of the instantaneous wind $V(t)$. The rules for defining the angles $\tilde{\beta}$ and $\tilde{\theta}$ are similar to those for the angles $\bar{\beta}$ and $\bar{\theta}$.

Figs. 3 and 4 show the local mean wind coordinates, the $\bar{q}\bar{p}\bar{h}$-system, and the local instantaneous wind coordinates, the $\tilde{q}\tilde{p}\tilde{h}$-system, respectively, which are used to derive the six-component buffeting forces acting on an oblique strip (element). The $\bar{q}\bar{p}\bar{h}$-system is attained by rotating the qph-system by an angle of $\bar{\beta}$ around the axis h first and then by an angle of $\bar{\theta}$ around the axis $\bar{q}$. Similarly, the $\tilde{q}\tilde{p}\tilde{h}$-system is attained by rotating the qph-system by an angle of $\tilde{\beta}$ around the axis h first and then by an angle of $\tilde{\theta}$ around the axis $\tilde{q}$. As a result, the axes $\bar{q}$ and $\tilde{q}$ are located in the qp-plane. The axis $\bar{p}$ is along the mean wind direction whilst the axis $\tilde{p}$ is along the instantaneous wind direction.

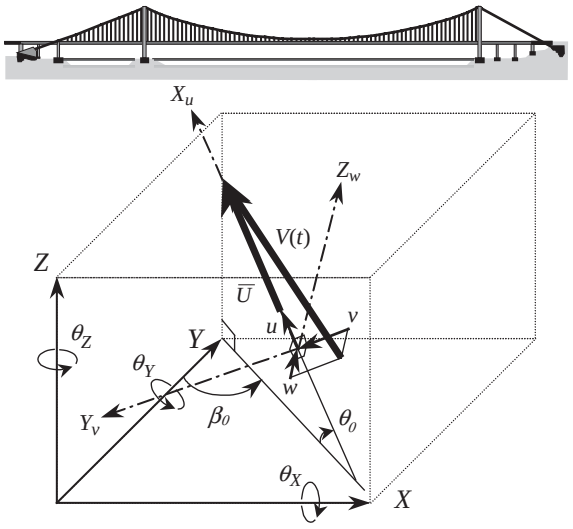

Fig. 1. Global structural and wind coordinate systems.

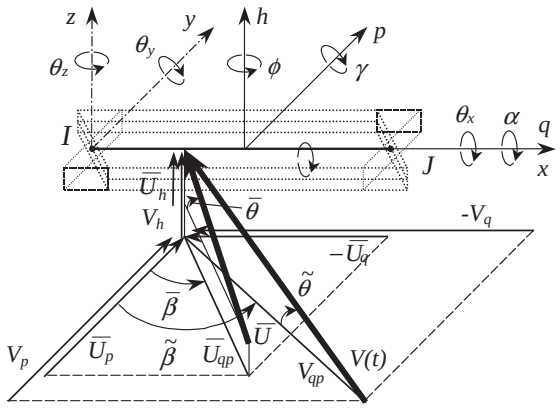

Fig. 2. Local reference coordinate system.

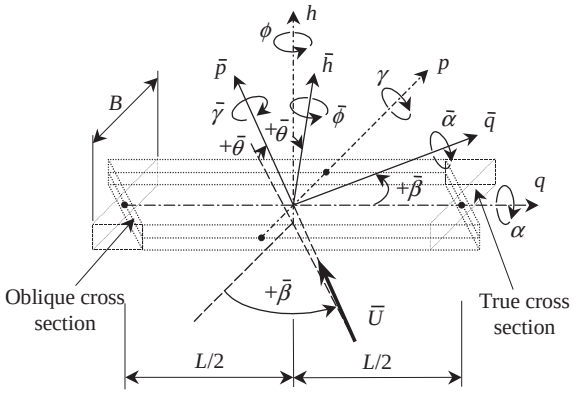

Fig. 3. Local mean wind coordinate system.

2.2. Transformation matrices between coordinate systems

In the following context, various coordinate transformation matrices are to be used during the formulation of buffeting forces. Denote by $\mathbf{T}_{S_1S_2}$ the 3×3 transformation matrix from the system S_2 to the system S_1, where the subscripts S_1 and S_2 ($S_1\neq S_2$) can be any two of G_W, G_S, L_s, L_r, $L_{\bar{w}}$ and $L_{\tilde{w}}$ which represents, respectively, the global wind coordinate $X_uY_vZ_w$-system, the global structural coordinate XYZ-system, the local structural coordinate xyz-system, the local reference coordinate qph-system, the local mean wind coordinate $\bar{q}\bar{p}\bar{h}$-system, and the local instantaneous wind coordinate $\tilde{q}\tilde{p}\tilde{h}$-system. $\bar{\mathbf{T}}_{S_1S_2}=\mathbf{Diag}(\mathbf{T}_{S_1S_2},\mathbf{T}_{S_1S_2})$ is then the 6×6 transformation matrix or $\hat{\mathbf{T}}_{S_1S_2}=\mathbf{Diag}(\mathbf{T}_{S_1S_2}\mathbf{T}_{S_1S_2}\mathbf{T}_{S_1S_2}\mathbf{T}_{S_1S_2})$ is the 12×12 transformation matrix. Here, **Diag** represents a diagonal matrix comprising the elements or sub-matrices in the parentheses. Clearly, if the dimension of the system S_3 is the same

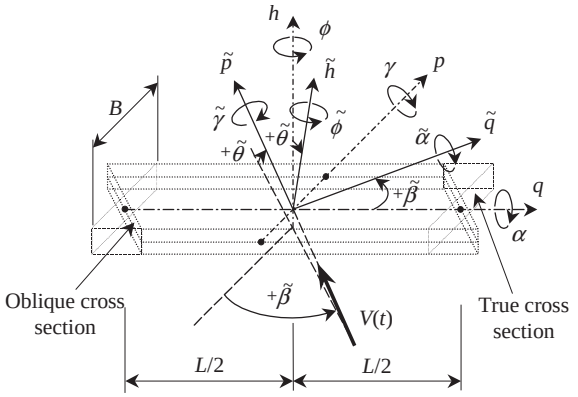

Fig. 4. Local instantaneous wind coordinate system.

as those of systems S_1 and S_2, then

$$\mathbf{T}_{S_1S_3} = \mathbf{T}_{S_1S_2}\mathbf{T}_{S_2S_3}. \tag{1}$$

For example, for the two global systems shown in Fig. 1, the transformation matrix can be expressed as

$$\mathbf{T}_{GsGw} = \mathbf{T}_{GwGs}^{\mathrm{T}} = \begin{bmatrix} -\cos\theta_0 \sin\beta_0 & -\cos\beta_0 & \sin\theta_0 \sin\beta_0 \\ \cos\theta_0 \cos\beta_0 & -\sin\beta_0 & -\sin\theta_0 \cos\beta_0 \\ \sin\theta_0 & 0 & \cos\theta_0 \end{bmatrix}. \tag{2}$$

The transformation matrix between the global wind coordinate system $X_uY_vZ_w$ and the local reference coordinate system *qph* can be found as

$$\mathbf{T}_{LrGw} = \mathbf{T}_{LrLs}\mathbf{T}_{LsGs}\mathbf{T}_{GsGw} = \begin{bmatrix} t_{11} & t_{12} & t_{13} \\ t_{21} & t_{22} & t_{23} \\ t_{32} & t_{32} & t_{33} \end{bmatrix}, \tag{3}$$

where t_{ij} ($i,j=1,2,3$) is the element of $\mathbf{T}_{LrGw}$ at the ith row and jth column, and it is the function of β_0 and θ_0. Moreover, one can derive the transformation matrix between the local mean wind coordinate system and the local reference coordinate system as

$$\mathbf{T}_{LrL\bar{w}} = \begin{bmatrix} \cos\bar{\beta} & -\cos\bar{\theta}\sin\bar{\beta} & \sin\bar{\theta}\sin\bar{\beta} \\ \sin\bar{\beta} & \cos\bar{\theta}\cos\bar{\beta} & -\sin\bar{\theta}\cos\bar{\beta} \\ 0 & \sin\bar{\theta} & \cos\bar{\theta} \end{bmatrix}. \tag{4}$$

The 6×6 transformation matrix from the local instantaneous wind coordinate system to the local mean wind coordinate system ($\mathbf{T}_{L\tilde{w}L\tilde{w}}$) can be expressed as

$$\bar{\mathbf{T}}_{L\tilde{w}L\tilde{w}} = \mathbf{I} + \bar{\mathbf{T}}_v \frac{v}{\bar{U}} + \bar{\mathbf{T}}_w \frac{w}{\bar{U}}, \tag{5}$$

where $\mathbf{I}$ is the 6×6 identity matrix, and

$$\bar{\mathbf{T}}_v = \begin{bmatrix} \mathbf{T}_v & \mathbf{0} \\ \mathbf{0} & \mathbf{T}_v \end{bmatrix}, \quad \mathbf{T}_v = \begin{bmatrix} 0 & -s_1 & s_2 t_{31} \\ s_1 & 0 & -s_3 \\ -s_2 t_{31} & s_3 & 0 \end{bmatrix}, \tag{6a}$$

$$\bar{\mathbf{T}}_w = \begin{bmatrix} \mathbf{T}_w & \mathbf{0} \\ \mathbf{0} & \mathbf{T}_w \end{bmatrix}, \quad \mathbf{T}_w = \begin{bmatrix} 0 & -s_4 & s_5 t_{31} \\ s_4 & 0 & -s_6 \\ -s_5 t_{31} & s_6 & 0 \end{bmatrix}, \tag{6b}$$

$$s_1 = (t_{11}t_{22} - t_{21}t_{12}) \Big/ \sqrt{t_{11}^2 + t_{21}^2}, \quad s_2 = (t_{11}t_{22} - t_{21}t_{12}) \Big/ \left(t_{11}^2 + t_{21}^2\right), \tag{7a}$$

$$\begin{aligned} s_3 &= t_{32} \Big/ \sqrt{t_{11}^2 + t_{21}^2}, \quad s_4 = (t_{11}t_{23} - t_{21}t_{13}) \Big/ \sqrt{t_{11}^2 + t_{21}^2}, \\ s_5 &= (t_{11}t_{23} - t_{21}t_{13}) \Big/ \left(t_{11}^2 + t_{21}^2\right), \quad s_6 = t_{33} \Big/ \sqrt{t_{11}^2 + t_{21}^2}. \end{aligned} \tag{7b}$$

2.3. Velocity fluations of wind turbulence

As shown in Fig. 1, the alongwind, lateral and upward components of wind turbulence, $u(t)$, $v(t)$, and $w(t)$, are defined as the three velocity fluctuations along the axes X_u, Y_v and Z_w, respectively, and their positive directions are consistent with those of the axes X_u, Y_v and Z_w. Thus, $u(t)$ is along the direction of mean wind ($\bar{U}$), $v(t)$ is horizontal and normal to the mean wind direction, and $w(t)$ is upward and normal to the mean wind direction. The resultant wind is therefore

$$V(t) = \sqrt{[\bar{U} + u(t)]^2 + v^2(t) + w^2(t)}. \tag{8}$$

2.4. Determination of local wind yaw and inclination angles

The aerodynamic coefficients and flutter derivatives (aeroelastic coefficients) of a bridge component are often measured via wind tunnel tests and are expressed as the functions of mean wind yaw angle and inclination angle with respect to the test sectional model [32–34]. There, the mean wind yaw angle and inclination angle refer to $\bar{\beta}$ and $\bar{\theta}$ of the sectional model and they may be different from the global ones of β_0 and θ_0. Therefore, to use correctly the measured

aerodynamic coefficients and flutter derivatives when determining wind-induced forces acting on an arbitrary element, $\bar{\beta}$ and $\bar{\theta}$ should be determined first. It is noted that, although the vector of wind speed shows its different appearances in the global structural coordinate system and the local reference coordinate system, the absolute wind speed and direction are actually independent of the used coordinate systems. Therefore, the angles $\bar{\beta}$ and $\bar{\theta}$ for each element can be computed from β_0 and θ_0 with the following trigonometric functions derived via the coordinate transformation.

$$\cos\bar{\theta} = \sqrt{t_{11}^2 + t_{21}^2}, \quad \sin\bar{\theta} = t_{31}, \tag{9a}$$

$$\cos\bar{\beta} = t_{21}\Big/\sqrt{t_{11}^2 + t_{21}^2}, \quad \sin\bar{\beta} = -t_{11}\Big/\sqrt{t_{11}^2 + t_{21}^2}. \tag{9b}$$

Furthermore, the increments of the local wind yaw angle and inclination due to the fluctuating wind velocities are needed when formulating the linear model of buffeting forces by using the Taylor's expansion formula. In consideration of the fact that the fluctuating wind components are much smaller than the mean wind speed, the increments of local wind yaw angle ($\Delta\beta = \tilde{\beta} - \bar{\beta}$) and local wind inclination angle ($\Delta\theta = \tilde{\theta} - \bar{\theta}$) can thus be expressed as the following linear functions of u, v, and w by using the Taylor's expansion formula and ignoring all the nonlinear terms of u, v, and w.

$$\Delta\theta \approx \sin\Delta\theta = \frac{t_{32}}{\sqrt{t_{11}^2 + t_{21}^2}}\frac{v}{\bar{U}} + \frac{t_{33}}{\sqrt{t_{11}^2 + t_{21}^2}}\frac{w}{\bar{U}} \tag{10a}$$

$$\Delta\beta \approx \sin\Delta\beta = \frac{t_{11}t_{22} - t_{12}t_{21}}{t_{11}^2 + t_{21}^2}\frac{v}{\bar{U}} + \frac{t_{11}t_{23} - t_{13}t_{21}}{t_{11}^2 + t_{21}^2}\frac{w}{\bar{U}}. \tag{10b}$$

2.5. Elemental buffeting forces per unit length

Fig. 5 shows an oblique strip (element) parallel to the mean wind direction. The vector of the total aerodynamic wind forces acting on an element per unit length, $\tilde{\mathbf{f}}^{\mathrm{ad}}(t)$, due to the instantaneous wind velocity $V(t)$, can be expressed as

$$\tilde{\mathbf{f}}^{\mathrm{ad}}(t) = \left(C_{\tilde{q}}^{\mathrm{ad}}(t), D_{\tilde{p}}^{\mathrm{ad}}(t), L_{\tilde{h}}^{\mathrm{ad}}(t), M_{\tilde{\alpha}}^{\mathrm{ad}}(t), M_{\tilde{\gamma}}^{\mathrm{ad}}(t), M_{\tilde{\phi}}^{\mathrm{ad}}(t)\right)^{\mathrm{T}} = \frac{1}{2}\rho V^2(t)\mathbf{B}\tilde{\mathbf{C}}(\tilde{\beta}, \tilde{\theta}), \tag{11}$$

where $C_{\tilde{q}}^{\mathrm{ad}}(t)$, $D_{\tilde{p}}^{\mathrm{ad}}(t)$, $L_{\tilde{h}}^{\mathrm{ad}}(t)$ are the total crosswind force, drag force and lift force, respectively, along the axis $\tilde{q}$, the axis $\tilde{p}$ and the axis $\tilde{h}$ of the $\tilde{q}\tilde{p}\tilde{h}$-system; and $M_{\tilde{\alpha}}^{\mathrm{ad}}(t)$, $M_{\tilde{\gamma}}^{\mathrm{ad}}(t)$ and $M_{\tilde{\phi}}^{\mathrm{ad}}(t)$ are, respectively, the total pitching moment, rolling moment and yawing moment around the axis $\tilde{q}$, the axis $\tilde{p}$ and the axis $\tilde{h}$, respectively (see Fig. 5), ρ is the air density, and

$$\mathbf{B} = \mathbf{Diag}(B, B, B, B^2, B^2, B^2) \tag{12}$$

in which B is the characteristic width of the elemental true cross-section normal to the longitudinal axis of the element. $\tilde{\mathbf{C}}(\tilde{\beta}, \tilde{\theta})$ is the aerodynamic coefficient vector corresponding to $\tilde{\beta}$ and $\tilde{\theta}$.

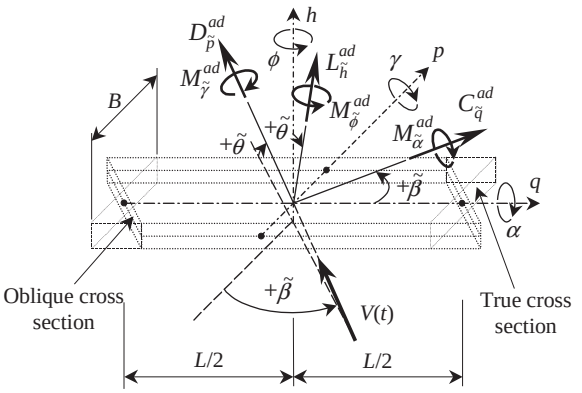

Fig. 5. Aerodynamic forces in local instantaneous wind coordinate system.

$\tilde{\mathbf{C}}(\tilde{\beta},\tilde{\theta})$ can be linearized by using the Taylor's formula and ignoring all nonlinear terms of u, v, and w.

$$\tilde{\mathbf{C}}(\tilde{\beta},\tilde{\theta}) = \bar{\mathbf{C}}(\bar{\beta},\bar{\theta}) + \bar{\mathbf{C}}'^{\beta}(\bar{\beta},\bar{\theta})\Delta\beta + \bar{\mathbf{C}}'^{\theta}(\bar{\beta},\bar{\theta})\Delta\theta, \tag{13}$$

where

$$\bar{\mathbf{C}}(\bar{\beta},\bar{\theta}) = \left(C_{C_{\tilde{q}}}, C_{D_{\tilde{p}}}, C_{L_{\tilde{h}}}, C_{M_{\tilde{\alpha}}}, C_{M_{\tilde{\gamma}}}, C_{M_{\tilde{\phi}}}\right)^{\mathrm{T}}_{(\bar{\beta},\bar{\theta})} \tag{14a}$$

is the aerodynamic coefficient vector corresponding to $\bar{\beta}$ and $\bar{\theta}$, and

$$\bar{\mathbf{C}}'^{\beta}(\bar{\beta},\bar{\theta}) = \partial\bar{\mathbf{C}}(\bar{\beta},\bar{\theta})/\partial\beta = \left(C'^{\beta}_{C_{\tilde{q}}}, C'^{\beta}_{D_{\tilde{p}}}, C'^{\beta}_{L_{\tilde{h}}}, C'^{\beta}_{M_{\tilde{\alpha}}}, C'^{\beta}_{M_{\tilde{\gamma}}}, C'^{\beta}_{M_{\tilde{\phi}}}\right)^{\mathrm{T}}_{(\bar{\beta},\bar{\theta})}, \tag{14b}$$

$$\bar{\mathbf{C}}'^{\theta}(\bar{\beta},\bar{\theta}) = \partial\bar{\mathbf{C}}(\bar{\beta},\bar{\theta})/\partial\theta = \left(C'^{\theta}_{C_{\tilde{q}}}, C'^{\theta}_{D_{\tilde{p}}}, C'^{\theta}_{L_{\tilde{h}}}, C'^{\theta}_{M_{\tilde{\alpha}}}, C'^{\theta}_{M_{\tilde{\gamma}}}, C'^{\theta}_{M_{\tilde{\phi}}}\right)^{\mathrm{T}}_{(\bar{\beta},\bar{\theta})} \tag{14c}$$

in which $C_{C_{\tilde{q}}}$, $C_{D_{\tilde{p}}}$,$C_{L_{\tilde{h}}}$, $C_{M_{\tilde{\alpha}}}$, $C_{M_{\tilde{\gamma}}}$and $C_{M_{\tilde{\phi}}}$ are, respectively, the aerodynamic coefficients of crosswind, drag and lift forces, and pitching, rolling and yawing momxents with respect to the local mean wind coordinate $\bar{q}\bar{p}\bar{h}$-system, the subscript $(\bar{\beta},\bar{\theta})$ means that the aerodynamic coefficients take the values at $\bar{\beta}$ and $\bar{\theta}$ based on the oblique strip, and $()'^{\beta} = \partial()/\partial\beta$ and $()'^{\theta} = \partial()/\partial\theta$ represent the partial derivatives with respect to either the local mean wind yaw angle or the local mean wind inclination.

As shown in Fig. 6, $C^b_{\tilde{q}}(t)$, $D^b_{\tilde{p}}(t)$, $L^b_{\tilde{h}}(t)$, $M^b_{\tilde{\alpha}}(t)$, $M^b_{\tilde{\gamma}}(t)$ and $M^b_{\tilde{\phi}}(t)$ are the buffeting crosswind, drag and lift forces, and pitching, rolling and yawing moments due to the fluctuating wind, with respect to the local mean wind coordinate $\bar{q}\bar{p}\bar{h}$-system, and the buffeting force vector can then be

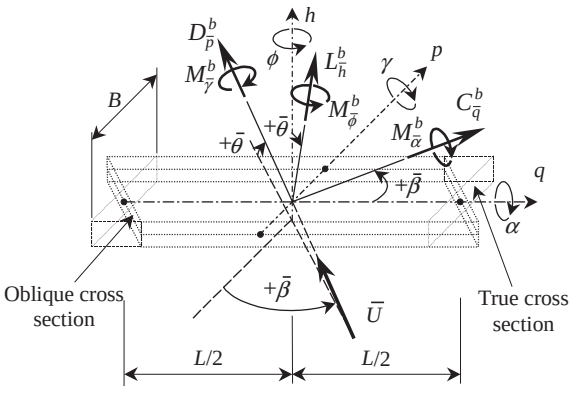

Fig. 6. Buffeting forces in local mean wind coordinate system.

expressed as

$$\bar{\mathbf{f}}^b(t) = \left(C_{\bar{q}}^b(t), D_{\bar{p}}^b(t), L_{\bar{h}}^b(t), M_{\bar{\alpha}}^b(t), M_{\bar{\gamma}}^b(t), M_{\bar{\phi}}^b(t)\right)^{\mathrm{T}} = \bar{\mathbf{T}}_{L\bar{w}L\tilde{w}}\tilde{\mathbf{f}}^{ad}(t) - \frac{1}{2}\rho\bar{U}^2\mathbf{B}\bar{\mathbf{C}}(\bar{\beta},\bar{\theta}), \tag{15}$$

where $\bar{\mathbf{T}}_{L\bar{w}L\tilde{w}}$ is determined by Eq. (5), $\Delta\beta$ and $\Delta\theta$ are determined by Eq. (10); $\tilde{\mathbf{f}}^{\mathrm{ad}}(t)$ is determined Eqs. (11)–(14). Then, by ignoring the nonlinear terms of $u(t)$, $v(t)$, and $w(t)$, one obtains

$$\bar{\mathbf{f}}^b(t) \approx \bar{\mathbf{A}}^b\bar{\mathbf{a}}(t), \tag{16}$$

where

$$\bar{\mathbf{a}}(t) = (u(t), v(t), w(t))^{\mathrm{T}} \tag{17}$$

and $\bar{\mathbf{A}}^b$ is the 6×3 aerodynamic coefficient matrix of buffeting forces, i.e.,

$$\bar{\mathbf{A}}^b = \left[\bar{\mathbf{A}}^u,\ \bar{\mathbf{A}}^v,\ \bar{\mathbf{A}}^w\right]. \tag{18a}$$

$$\bar{\mathbf{A}}^u = \rho\bar{U}\mathbf{B}\boldsymbol{\chi}_u(\bar{\beta},\bar{\theta},K)\bar{\mathbf{C}}(\bar{\beta},\bar{\theta}) = \frac{1}{2}\rho\bar{U}\left\{\begin{array}{c} 2C_{C_{\bar{q}}}B\chi_{C_{\bar{q}}u} \\ 2C_{D_{\bar{p}}}B\chi_{D_{\bar{p}}u} \\ 2C_{L_{\bar{h}}}B\chi_{L_{\bar{h}}u} \\ 2C_{M_{\bar{\alpha}}}B^2\chi_{M_{\bar{\alpha}}u} \\ 2C_{M_{\bar{\gamma}}}B^2\chi_{M_{\bar{\gamma}}u} \\ 2C_{M_{\bar{\phi}}}B^2\chi_{M_{\bar{\phi}}u} \end{array}\right\}_{(\bar{\beta},\bar{\theta})}, \tag{18b}$$

$$\bar{\mathbf{A}}^v = \frac{1}{2}\rho\bar{U}\Big\{\bar{\mathbf{T}}_v\mathbf{B}\boldsymbol{\chi}_v(\bar{\beta},\bar{\theta},K)\bar{\mathbf{C}}(\bar{\beta},\bar{\theta}) + s_2\mathbf{B}\boldsymbol{\chi}_v(\bar{\beta},\bar{\theta},K)\bar{\mathbf{C}}'^{\beta}(\bar{\beta},\bar{\theta}) + s_3\mathbf{B}\boldsymbol{\chi}_v(\bar{\beta},\bar{\theta},K)\bar{\mathbf{C}}'^{\theta}(\bar{\beta},\bar{\theta})\Big\}$$

$$= \frac{1}{2}\rho\bar{U}\begin{Bmatrix} [-s_1 C_{D_{\bar{p}}} + s_2 t_{31} C_{L_{\bar{h}}} + s_2 C'^{\beta}_{C_{\bar{q}}} + s_3 C'^{\theta}_{C_{\bar{q}}}] B\chi_{C_{\bar{q}}v} \\ [s_1 C_{C_{\bar{q}}} - s_3 C_{L_{\bar{h}}} + s_2 C'^{\beta}_{D_{\bar{p}}} + s_3 C'^{\theta}_{D_{\bar{p}}}] B\chi_{D_{\bar{p}}v} \\ [-s_2 t_{31} C_{C_{\bar{q}}} + s_3 C_{D_{\bar{p}}} + s_2 C'^{\beta}_{L_{\bar{h}}} + s_3 C'^{\theta}_{L_{\bar{h}}}] B\chi_{L_{\bar{h}}v} \\ [-s_1 C_{M_{\bar{\gamma}}} + s_2 t_{31} C_{M_{\bar{\phi}}} + s_2 C'^{\beta}_{M_{\bar{\alpha}}} + s_3 C'^{\theta}_{M_{\bar{\alpha}}}] B^2\chi_{M_{\bar{\alpha}}v} \\ [s_1 C_{M_{\bar{\alpha}}} - s_3 C_{M_{\bar{\phi}}} + s_2 C'^{\beta}_{M_{\bar{\gamma}}} + s_3 C'^{\theta}_{M_{\bar{\gamma}}}] B^2\chi_{M_{\bar{\gamma}}v} \\ [-s_2 t_{31} C_{M_{\bar{\alpha}}} + s_3 C_{M_{\bar{\gamma}}} + s_2 C'^{\beta}_{M_{\bar{\phi}}} + s_3 C'^{\theta}_{M_{\bar{\phi}}}] B^2\chi_{M_{\bar{\phi}}v} \end{Bmatrix}_{(\bar{\beta},\bar{\theta})}, \tag{18c}$$

$$\bar{\mathbf{A}}^{w} = \frac{1}{2}\rho\bar{U}\Big(\mathbf{T}_w\mathbf{B}\boldsymbol{\chi}_w(\bar{\beta},\bar{\theta},K)\bar{\mathbf{C}}(\bar{\beta},\bar{\theta}) + s_5\mathbf{B}\boldsymbol{\chi}_w(\bar{\beta},\bar{\theta},K)\bar{\mathbf{C}}'^{\beta}(\bar{\beta},\bar{\theta}) + s_6\mathbf{B}\boldsymbol{\chi}_w(\bar{\beta},\bar{\theta},K)\bar{\mathbf{C}}'^{\theta}(\bar{\beta},\bar{\theta})\Big)$$

$$= \frac{1}{2}\rho\bar{U}\begin{Bmatrix} [-s_4 C_{D_{\bar{p}}} + s_5 t_{31} C_{L_{\bar{h}}} + s_5 C'^{\beta}_{C_{\bar{q}}} + s_6 C'^{\theta}_{C_{\bar{q}}}] B\chi_{C_{\bar{q}}w} \\ [s_4 C_{C_{\bar{q}}} - s_6 C_{L_{\bar{h}}} + s_5 C'^{\beta}_{D_{\bar{p}}} + s_6 C'^{\theta}_{D_{\bar{p}}}] B\chi_{D_{\bar{p}}w} \\ [-s_5 t_{31} C_{C_{\bar{q}}} + s_6 C_{D_{\bar{p}}} + s_5 C'^{\beta}_{L_{\bar{h}}} + s_6 C'^{\theta}_{L_{\bar{h}}}] B\chi_{L_{\bar{h}}w} \\ [-s_4 C_{M_{\bar{\gamma}}} + s_5 t_{31} C_{M_{\bar{\phi}}} + s_5 C'^{\beta}_{M_{\bar{\alpha}}} + s_6 C'^{\theta}_{M_{\bar{\alpha}}}] B^2\chi_{M_{\bar{\alpha}}w} \\ [s_4 C_{M_{\bar{\alpha}}} - s_6 C_{M_{\bar{\phi}}} + s_5 C'^{\beta}_{M_{\bar{\gamma}}} + s_6 C'^{\beta}_{M_{\bar{\gamma}}}] B^2\chi_{M_{\bar{\gamma}}w} \\ [-s_5 t_{31} C_{M_{\bar{\alpha}}} + s_6 C_{M_{\bar{\gamma}}} + s_5 C'^{\beta}_{M_{\bar{\phi}}} + s_6 C'^{\theta}_{M_{\bar{\phi}}}] B^2\chi_{M_{\bar{\phi}}w} \end{Bmatrix}_{(\bar{\beta},\bar{\theta})} \tag{18d}$$

in which the coefficients s_i ($i=1,\ldots,6$) are determined by Eq. (7) and depend on β_0 and θ_0

$$\boldsymbol{\chi}_u(\bar{\beta},\bar{\theta},K) = \mathbf{Diag}(\chi_{C_{\bar{q}}u}, \chi_{D_{\bar{p}}u}, \chi_{L_{\bar{h}}u}, \chi_{M_{\bar{\alpha}}u}, \chi_{M_{\bar{\gamma}}u}, \chi_{M_{\bar{\phi}}u}), \tag{19a}$$

$$\boldsymbol{\chi}_v(\bar{\beta},\bar{\theta},K) = \mathbf{Diag}(\chi_{C_{\bar{q}}v}, \chi_{D_{\bar{p}}v}, \chi_{L_{\bar{h}}v}, \chi_{M_{\bar{\alpha}}v}, \chi_{M_{\bar{\gamma}}v}, \chi_{M_{\bar{\phi}}v}), \tag{19b}$$

$$\boldsymbol{\chi}_w(\bar{\beta},\bar{\theta},K) = \mathbf{Diag}(\chi_{C_{\bar{q}}w}, \chi_{D_{\bar{p}}w}, \chi_{L_{\bar{h}}w}, \chi_{M_{\bar{\alpha}}w}, \chi_{M_{\bar{\gamma}}w}, \chi_{M_{\bar{\phi}}w}). \tag{19c}$$

In the above equations, $K = \omega B/\bar{U}$ is the reduced frequency of the turbulence eddy with circular frequency ω; $\chi_{\bar{f}a}(\bar{\beta},\bar{\theta},K)$ ($\bar{f} = C_{\bar{q}}, D_{\bar{p}}, L_{\bar{h}}, M_{\bar{\alpha}}, M_{\bar{\gamma}}, M_{\bar{\phi}}$; $a = u, v, w$) are the 18 aerodynamic admittance functions, considering the unsteadiness of wind turbulence and the partial coherence of the turbulence along the chord of the oblique cross-section in skew wind direction [2,3]. All these aerodynamic admittance functions are the functions of the reduced frequency and the wind direction. The coherence of wind turbulence is higher for the turbulence components with longer wavelength (lower frequency or higher velocity) than for the turbulence components with shorter wavelength (higher frequency or lower velocity). As a result, the values of the aerodynamic admittance functions will drop with an increasing value of K.

Eqs. (16)–(19) are the universal expressions of the unit length quasi-steady buffeting forces acting on an arbitrary oblique element of the bridge deck, tower or cable due to skew winds. The conventional cases can be deducted from these expressions. For instance, if $\bar{\beta} = \beta_0 = 0$ and $\bar{\theta} = \theta_0 = 0$, all the values of $C_{C_{\bar{q}}}$, $C_{M_{\bar{\gamma}}}$, $C_{M_{\bar{\phi}}}$, and $C_{\bar{f}}^{'\beta}$ ($\bar{f} = C_{\bar{q}}$, $D_{\bar{p}}$, $L_{\bar{h}}$, $M_{\bar{\alpha}}$, $M_{\bar{\gamma}}$, $M_{\bar{\phi}}$) are zero for a straight element with constant cross-section, Eq. (18) can then be simplified as

$$\bar{\mathbf{A}}^b = \frac{1}{2}\rho\bar{U}\begin{bmatrix} 0 & -C_{D_{\bar{p}}}B\chi_{C_{\bar{q}}v} & 0 \\ 2BC_{D_{\bar{p}}}\chi_{D_{\bar{p}}u} & 0 & \left(-C_{L_{\bar{h}}} + C_{D_{\bar{p}}}^{'\theta}\right)B\chi_{D_{\bar{p}}w} \\ 2BC_{L_{\bar{h}}}\chi_{L_{\bar{h}}u} & 0 & \left(C_{D_{\bar{p}}} + C_{L_{\bar{h}}}^{'\theta}\right)B\chi_{L_{\bar{h}}w} \\ 2B^2C_{M_{\bar{\alpha}}}\chi_{M_{\bar{\alpha}}u} & 0 & C_{M_{\bar{\alpha}}}^{'\theta}B^2\chi_{M_{\bar{\alpha}}w} \\ 0 & C_{M_{\bar{\alpha}}}B^2\chi_{M_{\bar{\alpha}}v} & 0 \\ 0 & 0 & 0 \end{bmatrix}_{(0,0)} \tag{20}$$

which will be the same as that used in the traditional buffeting analysis of normal wind case when ignoring the lateral component of fluctuating wind.

2.6. Buffeting forces at element nodes

In the FE model of a long-span cable-supported bridge, the length of some elements, such as cable and tower leg elements, may be quite long. To ensure the accuracy of buffeting analysis, these elements can be further divided into a number of segments so that a constant mean and fluctuating wind speeds and a fully coherent turbulence wind can be assumed within each segment. Suppose that n_k is the total number of segments in the kth element ($k = 1, \ldots, M$), M is the number of elements of the entire bridge. $L_{i,k}$ ($i = 1, \ldots, n_k$) is the length of ith segment, according to the principle of virtual work, the 12 dimensional vector of buffeting forces at the nodes of the kth element, $\mathbf{f}_{e,k}^b(t)$, in the xyz-system can be derived as

$$\begin{aligned} \mathbf{f}_{e,k}^b(t) &= \left(F_{xI}^b, F_{yI}^b, F_{zI}^b, M_{\theta_{xI}}^b, M_{\theta_{yI}}^b, M_{\theta_{zI}}^b, F_{xJ}^b, F_{yJ}^b, F_{zJ}^b, M_{\theta_{xJ}}^b, M_{\theta_{yJ}}^b, M_{\theta_{zJ}}^b\right)_k^{\mathrm{T}} \\ &= L_k \int_0^1 \mathbf{N}_{\delta,k}^{\mathrm{T}}(\xi)\bar{\mathbf{T}}_{LsLr,k}\bar{\mathbf{T}}_{LrL\bar{w},k}\bar{\mathbf{A}}_k^b\bar{\mathbf{a}}_k(\xi,t)\,\mathrm{d}\xi \\ &= L_k \sum_{i=1}^{n_k}\left(\left[\bar{\mathbf{T}}_{LsLr,k}^{\mathrm{T}}\int_{\xi_{i-1,k}}^{\xi_{i,k}}\mathbf{N}_{\delta,k}(\xi)\,\mathrm{d}\xi\right]^{\mathrm{T}}\bar{\mathbf{T}}_{LrL\bar{w},k}\bar{\mathbf{A}}_{i,k}^b\bar{\mathbf{a}}_{i,k}(t)\right), \end{aligned} \tag{21}$$

where the subscript k indicates the kth element, the subscript i indicates the ith segment, I and J represent the left and right nodes of the element, $\xi = x/L_k$ ($0 \leqslant \xi \leqslant 1$) is the reduced coordinate, $\xi_{i,k} = x_{i,k}/L_k$, $L_k = \sum_{i=1}^{n_k} L_{i,k}$ is the total length of the kth element, and $x_{i,k}$ is the distance from the right end of the ith segment to the left node of the kth element with $x_{0,k} = 0$, $\mathbf{N}_{\delta,k}(\xi)$ is the 6×12 matrix of displacement interpolation function of the kth element with respect to the local xyz-system, reflecting the relationship between the displacement at an arbitrary position within the kth element and the nodal displacements.

Designate $\mathbf{F}_{e,k}^{b}(t)$ the 12 dimensional nodal buffeting force vector of the kth element in XYZ-system. It can then be obtained through the coordinate transformation as follows:

$$\begin{aligned}\mathbf{F}_{e,k}^{b}(t) &= \left(F_{XI}^{b}, F_{YI}^{b}, F_{ZI}^{b}, M_{\theta_{XI}}^{b}, M_{\theta_{YI}}^{b}, M_{\theta_{ZI}}^{b}, F_{XJ}^{b}, F_{YJ}^{b}, F_{ZJ}^{b}, M_{\theta_{XJ}}^{b}, M_{\theta_{YJ}}^{b}, M_{\theta_{ZJ}}^{b}\right)_{k}^{\mathrm{T}} \\ &= \hat{\mathbf{T}}_{GsLs,k}\mathbf{f}_{e,k}^{b}(t) = \sum_{i=1}^{n_k} \mathbf{P}_{i,k}^{b}\bar{\mathbf{a}}_{i,k}(t),\end{aligned} \tag{22}$$

where $\hat{\mathbf{T}}_{GsLs,k}$is the 12×12 transformation matrix of the kth element from the xyz-system to the XYZ-system; $\mathbf{P}_{i,k}^{b}(t)$ is the 12×3 coefficient matrix of nodal buffeting forces with respect to the XYZ-system for the ith segment of the kth element and is determined by

$$\mathbf{P}_{i,k}^{b} = L_k\hat{\mathbf{T}}_{GsLs,k}\left[\bar{\mathbf{T}}_{LsLr,k}^{\mathrm{T}}\int_{\xi_{i-1,k}}^{\xi_{i,k}}\mathbf{N}_{\delta,k}(\xi)\,\mathrm{d}\xi\right]^{\mathrm{T}}\bar{\mathbf{T}}_{LrL\bar{w},k}\bar{\mathbf{A}}_{i,k}^{b}. \tag{23}$$

2.7. Global buffeting force vector

Designate $\mathbf{F}^{b}(t)$ the $6N$-dimensional global vector of nodal buffeting forces of the entire bridge assembled in the XYZ-system, where N is the number of nodes in the FE model of the bridge. It can then be assembled from all $\mathbf{F}_{e,k}^{b}(t)$ and expressed as follows:

$$\mathbf{F}^{b}(t) = \mathbf{P}^{b}\mathbf{a}(t), \tag{24}$$

where $\mathbf{P}^{b}$ is the $6N\times 3m$ coefficient matrix of buffeting forces, assembled from all $\mathbf{P}_{i,k}^{b}(t)$, and it is frequency-dependent and complex in nature if aerodynamic admittance functions are included in the computation, m is the total number of segments of the entire bridge and also the total point number of random excitations of fluctuating wind, and $3m$ is the total number of the random excitations.

$$\mathbf{a}(t) = \left(\bar{\mathbf{a}}_{1,1}^{\mathrm{T}}, \ldots, \bar{\mathbf{a}}_{n_1,1}^{\mathrm{T}}, \ldots, \bar{\mathbf{a}}_{n_1,k}^{\mathrm{T}}, \ldots, \bar{\mathbf{a}}_{n_k,k}^{\mathrm{T}}, \ldots, \bar{\mathbf{a}}_{1,M}^{\mathrm{T}}, \ldots, \bar{\mathbf{a}}_{n_M,M}^{\mathrm{T}}\right)^{\mathrm{T}} \tag{25}$$

is a vector of the fluctuating wind components of the entire bridge and is of $3m$ dimensions.

2.8. Spectral density function matrix of global buffeting forces

The Fourier transformation of the buffeting force vector $\mathbf{F}^{b}(t)$ is

$$\widehat{\mathbf{F}}^{b}(\omega) = \mathbf{P}^{b}(\omega)\,\widehat{\mathbf{a}}(\omega), \tag{26}$$

where $\widehat{\mathbf{a}}(\omega)$ is the Fourier transformation of fluctuating wind vector $\mathbf{a}(t)$. By using the following relationship

$$\widehat{\mathbf{F}}^{b^*}(\omega)\widehat{\mathbf{F}}^{b^{\mathrm{T}}}(\omega) = \mathbf{P}^{b^*}(\omega)\widehat{\mathbf{a}}^{*}(\omega)\widehat{\mathbf{a}}^{\mathrm{T}}(\omega)\mathbf{P}^{b^{\mathrm{T}}}(\omega). \tag{27}$$

The spectral density function matrix of buffeting forces, $\mathbf{S}_{\mathrm{FF}}^{b}(\omega)$, can be gained as

$$\mathbf{S}_{\mathrm{FF}}^{b}(\omega) = \mathbf{P}^{b^*}(\omega)\mathbf{S}_{aa}(\omega)\mathbf{P}^{b^{\mathrm{T}}}(\omega), \tag{28}$$

where the superscript asterisk denotes a complex conjugation operation; $\mathbf{S}_{aa}(\omega)$ is the spectral density function matrix of fluctuating wind components. It is a $3m \times 3m$ matrix and can be expressed as follows:

$$\mathbf{S}_{aa}(\omega) = \begin{bmatrix} \mathbf{S}_{\bar{a}_{1,1}\bar{a}_{1,1}}(\omega) & \cdots & \mathbf{S}_{\bar{a}_{1,1}\bar{a}_{n_k,1}}(\omega) & \cdots & \mathbf{S}_{\bar{a}_{1,1}\bar{a}_{1,M}}(\omega) & \cdots & \mathbf{S}_{\bar{a}_{1,1}\bar{a}_{n_M,M}}(\omega) \\ \vdots & \ddots & \vdots & \ddots & \vdots & \ddots & \vdots \\ \mathbf{S}_{\bar{a}_{n_k,1}\bar{a}_{1,1}}(\omega) & \cdots & \mathbf{S}_{\bar{a}_{n_k,1}\bar{a}_{n_k,1}}(\omega) & \cdots & \mathbf{S}_{\bar{a}_{n_k,1}\bar{a}_{1,M}}(\omega) & \cdots & \mathbf{S}_{\bar{a}_{n_k,1}\bar{a}_{n_M,M}}(\omega) \\ \vdots & \ddots & \vdots & \ddots & \vdots & \ddots & \vdots \\ \mathbf{S}_{\bar{a}_{1,M}\bar{a}_{1,1}}(\omega) & \cdots & \mathbf{S}_{\bar{a}_{1,M}\bar{a}_{n_k,1}}(\omega) & \cdots & \mathbf{S}_{\bar{a}_{1,M}\bar{a}_{1,M}}(\omega) & \cdots & \mathbf{S}_{\bar{a}_{1,M}\bar{a}_{n_M,M}}(\omega) \\ \vdots & \ddots & \vdots & \ddots & \vdots & \ddots & \vdots \\ \mathbf{S}_{\bar{a}_{n_M,M}\bar{a}_{1,1}}(\omega) & \cdots & \mathbf{S}_{\bar{a}_{n_M,M}\bar{a}_{n_k,1}}(\omega) & \cdots & \mathbf{S}_{\bar{a}_{n_M,M}\bar{a}_{1,M}}(\omega) & \cdots & \mathbf{S}_{\bar{a}_{n_M,M}\bar{a}_{n_M,M}}(\omega) \end{bmatrix}, \quad (29a)$$

where $\mathbf{S}_{\bar{a}_{i,k}\bar{a}_{j,l}}(\omega)$ $(i = 1, \ldots, n_k;\ j = 1, \ldots, n_l;\ k = 1, \ldots, M,\ l = 1, \ldots, M)$ is the 3×3 matrix of auto/cross-spectral densities between the three fluctuating wind components at the center of the ith segment of the kth element as well as at the center of the jth segment of the lth element.

$$\mathbf{S}_{\bar{a}_{i,k}\bar{a}_{j,l}}(\omega) = \begin{bmatrix} S_{u_{i,k}u_{j,l}}(\omega) & S_{u_{i,k}v_{j,l}}(\omega) & S_{u_{i,k}w_{j,l}}(\omega) \\ S_{v_{i,k}u_{j,l}}(\omega) & S_{v_{i,k}v_{j,l}}(\omega) & S_{v_{i,k}w_{j,l}}(\omega) \\ S_{w_{i,k}u_{j,l}}(\omega) & S_{w_{i,k}v_{j,l}}(\omega) & S_{w_{i,k}w_{j,l}}(\omega) \end{bmatrix} \quad (29b)$$

in which, for example, $S_{v_{i,k}u_{j,l}}$ means the cross-spectrum between v at the center of the ith segment of the kth element and u at the center of the jth segment of the lth element. The diagonal elements of $\mathbf{S}_{aa}(\omega)$ are the auto-spectra of fluctuating wind at a designated location and they are real quantities. All the nondiagonal elements of $\mathbf{S}_{aa}(\omega)$ are the cross-spectra and complex in general with its real part being co-spectra of even function and its imaginary part being quadrature spectra of odd function. Thus, the double-side spectra $(-\infty < \omega < +\infty)$ are to be adopted in this study. In addition, it can be proved that $\mathbf{S}_{aa}(\omega)$ is a nonnegative definite Hermitian matrix [35].

The conventional expressions of cross-spectra between the fluctuating wind components at two different spatial points, P_1 and P_2, can be found frequently in the literature, such as those suggested in Refs. [14,36–40]. To carry out a fully coupled buffeting analysis of a 3D bridge, these conventional expressions are extended with the following forms, which take into account at the same time the turbulence coherence in all the three directions along the axes of the global wind coordinate $X_u Y_v Z_w$-system.

$$S_{a_{1P_1}a_{2P_2}}(\omega) = \sqrt{S_{a_{1P_1}a_{2P_1}}(\omega) S_{a_{1P2}a_{2P_2}}(\omega)}\, R_{a_{1P_1}a_{2P_2}}(\omega), \quad (30)$$

$$R_{a_{1P_1}a_{2P_2}}(\omega) = (1 - \hat{f}_{a_{1P_1}a_{2P_2}}) \exp\{-\hat{f}_{a_{1P_1}a_{2P_2}}(\omega) + \mathrm{i}\varphi_{a_{1P_1}a_{2P_2}}(\omega)\}, \quad (31)$$

$$\hat{f}_{a_{1P_1}a_{2P_2}}(\omega) = [\hat{f}_{a_{1P_1}a_{1P_2}}(\omega) + \hat{f}_{a_{2P_1}a_{2P_2}}(\omega)]/2, \quad (32a)$$

$$\hat{f}_{a_{P_1}a_{P_2}}(\omega)=\frac{2n_{xa}\sqrt{\left[C^a_{X_u}\left(X_{u_{P_1}}-X_{u_{P_2}}\right)\right]^2+\left[C^a_{Y_v}\left(Y_{v_{P_1}}-Y_{v_{P_2}}\right)\right]^2+\left[C^a_{Z_w}\left(Z_{w_{P_1}}-Z_{w_{P_2}}\right)\right]^2}}{\bar{U}_{P_1}+\bar{U}_{P_2}}, \tag{32b}$$

$$\varphi_{a_{1_{P_1}}a_{2_{P_2}}}(\omega)=\left[\varphi_{a_{1_{P_1}}a_{2_{P_2}}}(\omega)+\varphi_{a_{1_{P_1}}a_{2_{P_2}}}(\omega)\right]\Big/2, \tag{32c}$$

where each of the subscripts a, a_1, and a_2 can be one of u, v, and w; $R_{a_{1_{P_1}}a_{2_{P_2}}}$ is the root-coherence function between the fluctuating wind components a_1 at point P_1 and a_2 at point P_2; $\mathrm{i}=\sqrt{-1}$; $X_{u_{P_j}}$, $Y_{v_{P_j}}$ and $Z_{w_{P_j}}$ are the coordinates of point P_j ($j=1,2$) in the global wind coordinate $X_uY_vZ_w$-system; $\bar{U}_{P_j}$ is the mean wind speed at point P_j, determined by the specified design wind speed and mean wind profile; when $a_1\neq a_2$, $S_{a_{1_{P_j}}a_{2_{Pj}}}$ is the cross-spectrum between a_1 and a_2 at point P_j and it is a complex function of ω with a real part called the co-spectrum and a imaginary part called the quadrature spectrum, otherwise it is the auto-spectrum and a real function of ω; $C^a_{X_u}$, $C^a_{Y_v}$ and $C^a_{Z_w}$ are the 9 decay coefficients of turbulence coherence; $\varphi_{a_{1_{P_1}}a_{2_{P_2}}}$ is the phase spectrum between the turbulent component a_1 at point P_1 and the turbulent component a_2 at point P_2, and it is traditionally set to zero in practice because there is little information about it; and $n_{xa}$are the modified frequency determined by [14,37,39,40]

$$n_{xa}=\frac{\Gamma(5/6)}{2\sqrt{\pi}\Gamma(1/3)}\sqrt{1+70.78\left(\frac{nL^{x_u}_a}{\bar{U}(z)}\right)^2}\frac{\bar{U}(z)}{L^{x_u}_a}\approx\sqrt{n^2+\frac{1}{70.78}\left(\frac{\bar{U}(z)}{L^{x_u}_a}\right)^2}, \tag{33}$$

where $n=\omega/2\pi$ is the turbulence frequency, $L^{x_u}_a$ is the length scale of turbulence component a in the alongwind direction, and Γ represents the Gamma function.

3. Aeroelastic forces under skew winds

Fig. 7 shows an arbitrary oblique segment of the bridge element submerged in a skew wind field with the mean wind speed $\bar{U}$ and the local mean wind yaw angle $\bar{\beta}$ and inclination $\bar{\theta}$. When the segment oscillates due to wind, there will be some motion-dependent aeroelastic forces and moments acting on the segment caused by the interaction between the segment motion and the wind around the segment. These self-excited forces are often expressed in terms of the Scanlan's flutter derivatives [4,5,12,14,41]. Since this investigation concerns skew winds, the Scanlan's flutter derivatives are to be measured from the wind tunnel tests with an oblique sectional model under skew winds [34]. Thus, they are not only the function of the reduced frequency but also the function of $\bar{\beta}$ and $\bar{\theta}$. Theoretically, there should be six components of the aeroelastic forces/moments but only the three major components, i.e., the pitching moment M^{se}_{α}, drag D^{se}_{p} and lift L^{se}_{h}, as shown in Fig. 7, are generally regarded to be significant to the buffeting response prediction of the bridge.

In this study, the M^{se}_{α}, D^{se}_{p} and L^{se}_{h} are defined with respect to the *qph*-system rather than the $\bar{q}\bar{p}\bar{h}$-system because they are induced by structural motions. These are also consistent with the wind tunnel measurements of flutter derivatives described in the literature [34]. Thus, the positive directions of M^{se}_{α}, D^{se}_{p} and L^{se}_{h} are determined by the *qph*-system and independent of $\bar{\beta}$ and $\bar{\theta}$.

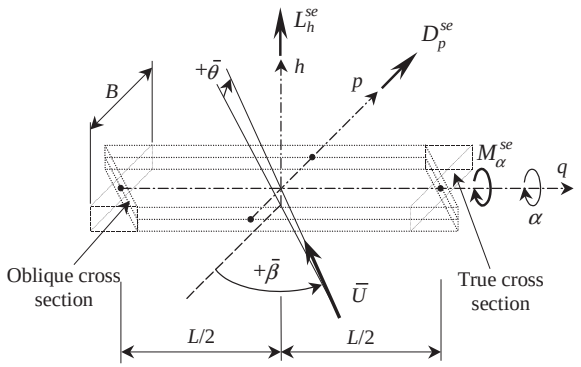

Fig. 7. Aeroelastic forces in local reference coordinate system.

Similar to that in Refs. [4,5,12,14,41], the following expressions are then adopted in this study for the self-excited aeroelastic forces acting on a unit length segment of a bridge component under skew winds:

$$M_\alpha^{se} = \frac{1}{2}\rho\bar{U}^2B^2\left[KA_1^*(\bar{\beta},\bar{\theta},K)\frac{\dot{\delta}_h}{\bar{U}} + KA_2^*(\bar{\beta},\bar{\theta},K)\frac{B\dot{\delta}_\alpha}{\bar{U}} + K^2A_3^*(\bar{\beta},\bar{\theta},K)\delta_\alpha + K^2A_4^*(\bar{\beta},\bar{\theta},K)\frac{\delta_h}{B} + KA_5^*(\bar{\beta},\bar{\theta},K)\frac{\dot{\delta}_p}{\bar{U}} + K^2A_6^*(\bar{\beta},\bar{\theta},K)\frac{\delta_p}{B}\right], \tag{34a}$$

$$D_p^{se} = \frac{1}{2}\rho\bar{U}^2B\left[KP_1^*(\bar{\beta},\bar{\theta},K)\frac{\dot{\delta}_p}{\bar{U}} + KP_2^*(\bar{\beta},\bar{\theta},K)\frac{B\dot{\delta}_\alpha}{\bar{U}} + K^2P_3^*(\bar{\beta},\bar{\theta},K)\delta_\alpha + K^2P_4^*(\bar{\beta},\bar{\theta},K)\frac{\delta_p}{B} + KP_5^*(\bar{\beta},\bar{\theta},K)\frac{\dot{\delta}_h}{\bar{U}} + K^2P_6^*(\bar{\beta},\bar{\theta},K)\frac{\delta_h}{B}\right], \tag{34b}$$

$$L_h^{se} = \frac{1}{2}\rho\bar{U}^2B\left[KH_1^*(\bar{\beta},\bar{\theta},K)\frac{\dot{\delta}_h}{\bar{U}} + KH_2^*(\bar{\beta},\bar{\theta},K)\frac{B\dot{\delta}_\alpha}{\bar{U}} + K^2H_3^*(\bar{\beta},\bar{\theta},K)\delta_\alpha + K^2H_4^*(\bar{\beta},\bar{\theta},K)\frac{\delta_h}{B} + KH_5^*(\bar{\beta},\bar{\theta},K)\frac{\dot{\delta}_p}{\bar{U}} + K^2H_6^*(\bar{\beta},\bar{\theta},K)\frac{\delta_p}{B}\right], \tag{34c}$$

where $\delta_p(t)$ and $\delta_h(t)$ are the dynamic displacements along the axis p and the axis h and $\delta_\alpha(t)$ is the dynamic angular displacement about the axis q, each over-dot denotes one order of partial differentiation with respect to time, and $P_i^*(\bar{\beta},\bar{\theta},K)$, $H_i^*(\bar{\beta},\bar{\theta},K)$ and $A_i^*(\bar{\beta},\bar{\theta},K)$ $(i=1,\ldots,6)$ are the flutter derivatives of the oblique cross-section in the mean wind direction, and they take the width of the true cross-section (B) as the referenced characteristic width (see Fig. 7 and Ref. [34]).

Finally, the global vector of self-excited aeroelastic forces of the whole bridge, $\mathbf{F}^{se}(t)$, can be expressed as

$$\mathbf{F}^{se}(t) = -\mathbf{K}^{se}\boldsymbol{\Delta}(t) - \mathbf{C}^{se}\dot{\boldsymbol{\Delta}}(t). \tag{35}$$

where $\mathbf{K}^{se}$ and $\mathbf{C}^{se}$ are the $6N \times 6N$ global aerodynamic stiffness matrix and damping matrix with respect to the XYZ-system, which can be easily obtained based on Eq. (34) according to the finite element technique. $\mathbf{\Delta}(t)$ is the $6N$-dimensional vector of the nodal displacement of the whole bridge referring to the XYZ-system.

4. Governing equation and solution

Under the framework of finite element approach, the governing equation for buffeting analysis of a long-span cable-supported bridge under skew winds can be expressed as

$$\mathbf{M}\ddot{\mathbf{\Delta}}(t) + \mathbf{C}\dot{\mathbf{\Delta}}(t) + \mathbf{K}\mathbf{\Delta}(t) = \mathbf{F}^{b}(t), \tag{36}$$

where

$$\mathbf{M} = \mathbf{M}^{s}, \quad \mathbf{K} = \mathbf{K}^{s} + \mathbf{K}^{se}, \quad \mathbf{C} = \mathbf{C}^{s} + \mathbf{C}^{se}, \tag{37}$$

where $\mathbf{M}^{s}$, $\mathbf{C}^{s}$ and $\mathbf{K}^{s}$ are, respectively, the global structural mass, damping and stiffness matrices of the whole bridge with the dimensions of $6N \times 6N$, $\mathbf{F}^{b}(t)$ is the $6N$-dimensional buffeting force vector of the entire bridge under skew winds, which are determined by Eq. (24).

Because the number of degrees of freedom (dof) of the FE model of a long-span bridge is very large, the modal superposition scheme is commonly used to reduce computational efforts when solving the governing equation in the frequency domain. Traditionally, the complete quadratic combination (CQC) method and the square root of the sum of square (SRSS) method are employed for the solution [42,43]. However, the CQC method needs great computational efforts for its high accuracy while the SRSS method bears the loss of accuracy to some extent for its facility. In this connection, a so-called pseudo-excitation method developed by Lin et al. [13,16,44–46] is used in this study to solve the governing equation (36) with less computational efforts and, at the same time, of enough accuracy.

Designating $\mathbf{\Phi}$ the $6N \times M_{\Phi}$ modal matrix containing the M_{Φ} modes of vibration of the entire bridge and introducing the following linear transformation for the buffeting displacement response of the bridge.

$$\mathbf{\Delta}(t) = \mathbf{\Phi}\boldsymbol{\eta}(t) = [\boldsymbol{\phi}_1, \ldots, \boldsymbol{\phi}_r, \ldots, \boldsymbol{\phi}_{M_{\Phi}}]\boldsymbol{\eta}(t), \tag{38}$$

where $\boldsymbol{\phi}_r$ is the $6N \times 1$ mode shape vector of the rth mode; and $\boldsymbol{\eta}(t)$ is the $M_{\Phi} \times 1$ vector of generalized displacement coordinates, Eq. (36) can be reduced to

$$\tilde{\mathbf{M}}^{s}\ddot{\boldsymbol{\eta}}(t) + (\tilde{\mathbf{C}}^{s} + \tilde{\mathbf{C}}^{se})\dot{\boldsymbol{\eta}}(t) + (\tilde{\mathbf{K}}^{s} + \tilde{\mathbf{K}}^{se})\boldsymbol{\eta}(t) = \tilde{\mathbf{F}}^{b}(t), \tag{39}$$

where $\tilde{\mathbf{F}}^{b}(t)$ is the $M_{\Phi} \times 1$ vector of the generalized buffeting force, determined using the following equations.

$$\tilde{\mathbf{F}}^{b}(t) = \mathbf{\Phi}^{\mathrm{T}}\mathbf{F}^{b}(t) = \mathbf{\Phi}^{\mathrm{T}}\mathbf{P}^{b}\mathbf{a}(t), \tag{40}$$

where $\tilde{\mathbf{M}}^{s}$, $\tilde{\mathbf{K}}^{s}$, $\tilde{\mathbf{C}}^{s}$, $\tilde{\mathbf{K}}^{se}$ and $\tilde{\mathbf{C}}^{se}$ are, respectively, the diagonal matrices of the generalized structural mass, stiffness and damping, and the generalized aerodynamic stiffness and damping matrices

with dimensions of $M_\Phi \times M_\Phi$.

$$\tilde{\mathbf{M}}^s = \mathbf{\Phi}^{\mathrm{T}}\mathbf{M}^s\mathbf{\Phi}, \tag{41}$$

$$\tilde{\mathbf{C}}^s = \mathbf{\Phi}^{\mathrm{T}}\mathbf{C}^s\mathbf{\Phi} = \tilde{\mathbf{M}}^s\,\mathbf{Diag}(2\zeta_1\omega_1,\ldots,2\zeta_{M_\Phi}\omega_{M_\Phi}), \quad \tilde{\mathbf{C}}^{\mathrm{se}} = \mathbf{\Phi}^{\mathrm{T}}\mathbf{C}^{\mathrm{se}}\mathbf{\Phi}, \tag{42}$$

$$\tilde{\mathbf{K}}^s = \mathbf{\Phi}^{\mathrm{T}}\mathbf{K}^s\mathbf{\Phi} = \tilde{\mathbf{M}}^s\mathbf{Diag}\,(\omega_1^2,\ldots,\omega_{M_\Phi}^2), \quad \tilde{\mathbf{K}}^{\mathrm{se}} = \mathbf{\Phi}^{\mathrm{T}}\mathbf{K}^{\mathrm{se}}\mathbf{\Phi}, \tag{43}$$

where ω_r and ζ_r $(r = 1,\ldots,M_\Phi)$ are the natural circular frequency and damping ratio, respectively, of the rth mode of vibration of the bridge.

Provided that the fluctuating wind components in the vector $\mathbf{a}(t)$ are stationary random processes and the bridge vibration is linear, $\tilde{\mathbf{F}}^b(t)$, $\boldsymbol{\eta}(t)$ and $\boldsymbol{\Delta}(t)$ are also stationary random processes. In accordance with random vibration theory [42,47], the cross-spectral density matrices of $\boldsymbol{\eta}(t)$ and $\boldsymbol{\Delta}(t)$ can be found from the cross-spectral density matrix $\mathbf{S}_{aa}(\omega)$ of the wind excitation as follows

$$\mathbf{S}_{\eta\eta}(\omega) = \tilde{\mathbf{H}}^*(\omega)\mathbf{S}_{\tilde{\mathrm{F}}\tilde{\mathrm{F}}}(\omega)\tilde{\mathbf{H}}^{\mathrm{T}}(\omega), \quad \mathbf{S}_{\Delta\Delta}(\omega) = \mathbf{\Phi}\mathbf{S}_{\eta\eta}(\omega)\mathbf{\Phi}^{\mathrm{T}} \tag{44}$$

$$\mathbf{S}^b_{\tilde{\mathrm{F}}\tilde{\mathrm{F}}}(\omega) = \mathbf{\Phi}^{\mathrm{T}}\mathbf{P}^{b*}\mathbf{S}_{aa}(\omega)\mathbf{P}^{b\mathrm{T}}\mathbf{\Phi} \tag{45}$$

where $\mathbf{S}^b_{\tilde{\mathrm{F}}\tilde{\mathrm{F}}}(\omega)$ is the $M_\Phi \times M_\Phi$ matrix of the generalized buffeting force spectra, and the generalized matrix of frequency response function of the bridge is

$$\tilde{\mathbf{H}}(\omega) = \left[\left(\tilde{\mathbf{K}}^s + \tilde{\mathbf{K}}^{\mathrm{se}} - \omega^2\tilde{\mathbf{M}}^s\right) + \mathrm{i}\omega\left(\tilde{\mathbf{C}}^s + \tilde{\mathbf{C}}^{\mathrm{se}}\right)\right]^{-1}. \tag{46}$$

A direct computation of Eq. (44) is very time-consuming. However, because the cross-spectral matrix of wind turbulence, $\mathbf{S}_{aa}(\omega)$ is a nonnegative definite Hermitian matrix [35], it can be expressed as the sum of sub-spectral matrices using the $\mathbf{L}^*\mathbf{D}\mathbf{L}^{\mathrm{T}}$ decomposition as follows

$$\mathbf{S}_{aa}(\omega) = \mathbf{l}^*(\omega)\mathbf{d}(\omega)\mathbf{l}^{\mathrm{T}}(\omega) = \sum_{j=1}^{m_p}\mathbf{S}_{aa,j}(\omega), \quad \mathbf{S}_{aa,j}(\omega) = d_j\mathbf{l}_j^*(\omega)\mathbf{l}_j^{\mathrm{T}}(\omega), \tag{47}$$

where $m_p \leqslant 3m$ is the rank of the spectral matrix $\mathbf{S}_{aa}(\omega)$, $\mathbf{d}(\omega)$ is a $3m \times 3m$ real diagonal matrix, $\mathbf{l}(\omega)$ is a $3m \times 3m$ lower triangular matrix with all its diagonal elements being unity, $d_j(\omega)$ is the jth nonzero diagonal element of $\mathbf{d}(\omega)$, and $\mathbf{l}_j(\omega)$ is the jth column of $\mathbf{l}(\omega)$. As a result, Eq. (45) becomes

$$\mathbf{S}^b_{\tilde{\mathrm{F}}\tilde{\mathrm{F}}} = \sum_{j=1}^{m_p} d_j\tilde{\mathbf{l}}_j^*(\omega)\tilde{\mathbf{l}}_j^T(\omega), \quad \tilde{\mathbf{l}}_j(\omega) = \mathbf{\Phi}^{\mathrm{T}}\mathbf{P}^{\mathrm{b}}(\omega)\mathbf{l}_j(\omega). \tag{48}$$

Obviously, the generalized spectral matrix $\mathbf{S}^b_{\tilde{\mathrm{F}}\tilde{\mathrm{F}}}(\omega)$ is also Hermitian, and it can also be decomposed with $\mathbf{L}^*\mathbf{D}\mathbf{L}^{\mathrm{T}}$ as follows

$$\mathbf{S}^b_{\tilde{\mathrm{F}}\tilde{\mathrm{F}}}(\omega) = \mathbf{L}^*(\omega)\mathbf{D}(\omega)\mathbf{L}^{\mathrm{T}}(\omega) = \sum_{r=1}^{M_p} D_r(\omega)\mathbf{L}_r^*(\omega)\mathbf{L}_r^{\mathrm{T}}(\omega), \tag{49}$$

where $M_p \leqslant M_\Phi$ is the rank of $\mathbf{S}^b_{\tilde{\mathrm{F}}\tilde{\mathrm{F}}}(\omega)$; $\mathbf{D}(\omega)$ is a real $M_\Phi \times M_\Phi$ diagonal matrix, $\mathbf{L}(\omega)$ is a $M_\Phi \times M_\Phi$ lower triangular matrix with all its diagonal elements being unity, $D_r(\omega)$ is the rth nonzero diagonal element of $\mathbf{D}(\omega)$, and $\mathbf{L}_r(\omega)$ is the rth column of $\mathbf{L}(\omega)$. Physically, $\sqrt{D_r}\mathbf{L}_r(\omega)\mathrm{e}^{\mathrm{i}\omega t}$

can be regarded as a harmonic generalized pseudo-excitation of the generalized system governed by Eq. (39). One can then get

$$\tilde{\mathbf{M}}\ddot{\boldsymbol{\eta}}_{p,r}(\omega,t)+\tilde{\mathbf{C}}\dot{\boldsymbol{\eta}}_{p,r}(\omega,t)+\tilde{\mathbf{K}}\boldsymbol{\eta}_{p,r}(\omega,t)=\sqrt{D_r}\mathbf{L}_r(\omega)\mathrm{e}^{\mathrm{i}\omega t} \tag{50}$$

in which $\boldsymbol{\eta}_{p,r}(\omega,t)$ is the rth harmonic generalized pseudo-displacement response vector corresponding to the rth harmonic generalized pseudo-wind excitation. Since this is a determinate dynamic problem, the generalized pseudo-displacement response can be easily found as follows

$$\boldsymbol{\eta}_{p,r}(\omega,t)=\tilde{\mathbf{H}}(\omega)\mathbf{L}_r(\omega)\sqrt{D_r(\omega)}\mathrm{e}^{\mathrm{i}\omega t}. \tag{51}$$

Then, according to the principle of pseudo-excitation method [13,16,44–46], the cross-spectral matrices of the generalized buffeting response can be found as follows

$$\mathbf{S}_{\eta\eta}(\omega)=\sum_{r=1}^{M_p}\boldsymbol{\eta}^{*}_{p,r}(\omega,t)\boldsymbol{\eta}^{\mathrm{T}}_{p,r}(\omega,t)=\sum_{r=1}^{M_p}D_r(\omega)\tilde{\mathbf{H}}^{*}(\omega)\mathbf{L}^{*}_r(\omega)\mathbf{L}^{\mathrm{T}}_r(\omega)\tilde{\mathbf{H}}^{\mathrm{T}}(\omega). \tag{52}$$

From Eq. (44), one can then obtain the cross-spectral matrices of buffeting response as

$$\mathbf{S}_{\Delta\Delta}(\omega)=\sum_{r=1}^{M_p}D_r(\omega)\tilde{\boldsymbol{\Delta}}^{*}_{p,r}(\omega)\tilde{\boldsymbol{\Delta}}^{T}_{p,r}(\omega), \tag{53}$$

$$\tilde{\boldsymbol{\Delta}}_{p,r}(\omega)=\boldsymbol{\Phi}\tilde{\mathbf{H}}(\omega)\mathbf{L}_r(\omega). \tag{54}$$

Furthermore, the rms responses of the nodal displacement, velocity and acceleration can be calculated through the integral of corresponding spectrum in the frequency domain.

$$\boldsymbol{\sigma}_{\boldsymbol{\Delta}_i}=\sqrt{2\int_0^{+\infty}\mathbf{S}_{\boldsymbol{\Delta}_i}(\omega)\,\mathrm{d}\omega}, \tag{55}$$

where $\boldsymbol{\Delta}_i=(x_i,y_i,z_i,\theta_{xi},\theta_{yi},\theta_{zi})^{\mathrm{T}}$ and $\boldsymbol{\sigma}_{\boldsymbol{\Delta}_i}$ are the nodal displacement vector and the rms response vector of the nodal displacement at the ith node, respectively, $\mathbf{S}_{\boldsymbol{\Delta}_i}$ is auto-spectral vector of $\boldsymbol{\Delta}_i$ extracted from the diagonal elements of $\mathbf{S}_{\Delta\Delta}(\omega)$.

It is noticed that, except for the cases of very low frequency, the value of the cross-spectra between two turbulence components at two spatial points decreases rapidly with the increase of the distance between the two points. Therefore, $\mathbf{S}_{aa}(\omega)$, the cross-spectral matrix of wind turbulence, will be very sparse and of narrow band if the sequence of wind excitations (or elemental segments) is properly rearranged and all the cross-spectra with values lower than a sufficiently small number are ignored. Then, to promote the computing efficiency, only the elements within the narrow-band are computed, and any operation associated with the matrix elements, such as those in $\mathbf{L}^{*}\mathbf{D}\mathbf{L}^{\mathrm{T}}$ decomposition or in matrix multiplication, is carried out only for those significant element within the narrow band. A detailed comparison of computational efficiency between the traditional CQC method and the pseudo-excitation method shows that the pseudo-excitation method is much more efficient than the traditional CQC method [16].

5. Application

The effect of skew winds on the buffeting response of a long-span cable-supported bridge was investigated by applying the foregoing FE based framework to Tsing Ma Bridge in Hong Kong as a case study [48]. To this end, the buffeting responses of Tsing Ma Bridge were analyzed for a wide combination of wind yaw angle from -30° to 30° at an interval of 2° and wind inclination from -5° to 5° at an interval of 0.5°. The analysis results, consistent with those of wind tunnel tests [24–29] in general, show that the variations of buffeting responses are not monotonous with wind yaw angle and inclination, and the normal wind case may not be the worst case. Within the concerned range of wind direction, the worst wind directions are $\pm 12^\circ$ of yaw angle and 4° of inclination for the deck vertical response, 5° of yaw angle and -2.5° of inclination for the deck lateral response, and 0° of yaw angle and -2° of inclination for the deck torsional response. The deck lateral response is not sensitive to wind yaw angle within a range larger than $[-15^\circ, 15^\circ]$. For the 4° inclination, the deck vertical responses at $\pm 12^\circ$ yaw angle are about 1.15 times of that at 0° yaw angle. The variation pattern of the deck torsional response vs. yaw angle is largely depends on the inclination angle.

6. Concluding remarks

A new finite element based method for buffeting analysis of long-span cable-supported bridges under skew winds has been developed in the frequency domain utilizing the quasi-steady linear theory and the oblique strip theory in conjunction with the pseudo-excitation method. Major features of this method are summarized as follows:

(1) The new method is capable of predicting the fully coupled buffeting response of long-span cable-supported bridges under skew winds with acceptable computation efforts. The buffeting response predicted by the proposed method naturally includes the multi-mode and spatial mode effects, the effects of inter-mode coupling and aerodynamic coupling as well as the interaction among major bridge components.
(2) A set of universal expressions for six buffeting forces (moments) associated with an oblique strip along the mean wind speed has been derived. These buffeting forces are formed with respect to the local wind coordinate system and then converted to those with respect to the structural coordinate system. Thus, the skew mean wind and three orthogonal fluctuating wind components can be easily handled without any further decomposition. The set of universal expressions is applicable to all structural members including the bridge deck, cables and towers.
(3) Aerodynamic stiffness and damping matrices due to self-excited forces are taken into consideration in the proposed method by introducing the 18 flutter derivatives with respect to an oblique strip.
(4) By using the proposed method, the variations of mean wind speed, turbulence intensity, and auto-spectrum along the bridge longitudinal axis can be easily included in the buffeting prediction. The coherence of wind turbulence between any two arbitrary spatial points is considered in the global wind coordinate system rather than the global structural coordinate system.

(5) The developed FE method was applied to Tsing Ma Bridge to investigate the effects of skew winds on its buffeting response. The results is consistent with those of wind tunnel tests in general, and show that the variations of buffeting responses are not monotonous with wind yaw angle and inclination, and the normal wind case may not correspond with the worst case scenario.

A comparison between the computed and field-measured buffeting responses of Tsing Ma Bridge under skew wind during Typhoon Sam will be reported in Part 2 of this paper, which serves as a good instance for the verification of the proposed FE method.

Acknowledgments

The work described in this paper is financially supported by the Research Grants Council of Hong Kong (Project No. PolyU 5027/98E) and The Hong Kong Polytechnic University through its Area of Strategic Development Programme in Wind Effects on Structures, to which the writers are most grateful. The work is also a part of a research project financially supported by the National Natural Science Foundation of China (Project No. 50378068). Sincere thanks should go to Prof. H.F. Xiang of State Key Laboratory for Disaster Reduction in Civil Engineering at Tongji University, China, for his generous support and invaluable advice. The writers also want to thank Mr. M.C.H. Hui for improving the English of this paper. Any opinion and concluding remarks presented in this paper are entirely those of the writers.

References

[1] A.G. Davenport, The application of statistical concepts to the wind loading of structures, *Proceedings of the Institution of Civil Engineers, London* 19 (1961) 449–472.
[2] A.G. Davenport, The response of slender, line-like structures to a gusty wind, *Proceedings of the Institution of Civil Engineers, London* 23 (1962) 389–407.
[3] A.G. Davenport, Buffeting of a suspension bridge by storm winds, *Journal of the Structural Division ASCE* 88 (ST3) (1962) 233–268.
[4] R.H. Scanlan, R.H. Gade, Motion of suspension bridge spans under gusty wind, *Journal of the Structural Division ASCE* 103 (ST9) (1977) 1867–1883.
[5] R.H. Scanlan, The action of flexible bridge under wind, II: buffeting theory, *Journal of Sound and Vibration* 60 (2) (1978) 201–211.
[6] Y. K. Lin, Stochastic analysis of bridge motion in large-scale turbulent winds, *Proceedings of the Fifth International Conference on Wind Engineering*, Vol. 2, Fort Collins, Colorado, USA, 3, 1979, pp. 887–897.
[7] Y.K. Lin, Motion of suspension bridges in turbulent winds, *Journal of the Engineering Mechanics Division ASCE* 105 (EM6) (1979) 921–932.
[8] Y.K. Lin, J.N. Yang, Multimode bridge response to wind excitation, *Journal of Engineering Mechanics, ASCE* 109 (2) (1983) 586–603.
[9] G. Diana, F. Cheli, M. Bocciolone, Suspension bridge response to turbulent wind: comparison of a new numerical simulation method results with full scale data, *Proceedings of the Tenth International Conference on Wind Engineering: Wind Engineering into 21st Century,* Copenhagen, Denmark, 1999, pp. 871–878.
[10] V. Boonyapinyo, T. Miyata, H. Yamada, Advanced Aerodynamic analysis of suspension bridges by state-space approach, *Journal of Structural Engineering ASCE* 125 (12) (1999) 1357–1366.

[11] X. Chen, M. Matsumoto, A. Kareem, Time domain flutter and buffeting response analysis of bridges, *Journal of Engineering Mechanics ASCE* 126 (1) (2000) 7–16.
[12] A. Jain, N.P. Jones, R.H. Scanlan, Coupled buffeting analysis of long-span bridges, *Journal of Structural Engineering ASCE* 122 (7) (1996) 716–725.
[13] Y.L. Xu, D.K. Sun, J.M. Ko, J.H. Lin, Buffeting analysis of long span bridges: a new algorithm, *Computers and Structures* 68 (1998) 303–313.
[14] H. Katsuchi, N.P. Jones, R.H. Scanlan, Multimode coupled flutter and buffeting analysis of the Akashi-Kaikyo bridge, *Journal of Structural Engineering* 125 (1) (1999) 60–70.
[15] X.Z. Chen, M. Matsumoto, A. Kareem, Aerodynamic coupled effects on flutter and buffeting of bridges, *Journal of Engineering Mechanics ASCE* 126 (1) (2000) 17–26.
[16] D.K. Sun, Three Dimensional Wind-induced Vibration Analysis of Long-span Bridges, PhD Thesis, Dalian University of Technology, China, 1999 (in Chinese).
[17] Y.L. Xu, D.K. Sun, J.M. Ko, J.H. Lin, Fully coupled buffeting analysis of Tsing Ma suspension bridge, *Journal of Wind Engineering and Industrial Aerodynamics* 85 (1) (2000) 97–117.
[18] Y.L. Xu, L.D. Zhu, K.Y. Wong, K.W.Y. Chan, Field measurement results of Tsing Ma suspension bridge during Typhoon Victor, *Structural Engineering Mechanics* 10 (6) (2000) 454–559.
[19] L.D. Zhu, Y.L. Xu, F. Zhang, H.F. Xiang, Buffeting of a long suspension bridge: analysis and field measurement, *Proceedings of SPIE Sixth Annual International Symposium on NDE for Health Monitoring and Diagnostics,* Newport Beach, California, USA, 2001, pp. 323–334.
[20] J. Xie, H. Tanaka, Buffeting analysis of long span bridges to turbulent wind with yaw angle, *Journal of Wind Engineering and Industrial Aerodynamics* 37 (1) (1991) 65–77.
[21] K. Kimura, H. Tanaka, Bridge buffeting due to wind with yaw angles, *Journal of Wind Engineering and Industrial Aerodynamics* 41-44 (1992) 1309–1320.
[22] K. Kimura, S. Nakamura, H. Tanaka, Buffeting analysis for cable-stayed bridges during construction in yawed wind, *Proceedings of Symposium on Cable-stayed and Suspension Bridges*, Vol. 2, Deauville, France, 1994, pp. 109–116.
[23] R.H. Scanlan, Bridge buffeting by skew winds in erection stages, *Journal of Engineering Mechanics ASCE* 11 (2) (1993) 251–269.
[24] K. Kimura, T. Ohara, Lateral sway buffeting of bridge decks due to yawed wind, *Proceedings of the Tenth International Conference on Wind Engineering: Wind Engineering into 21st Century,* Copenhagen, Denmark, 1999, pp. 919–927.
[25] A.G. Davenport, N. Isyumov, D.J. Fader, C.E.P. Bowen, A study of wind action on a suspension bridge during erection and on completion: the narrows bridge, Halifax, Canada, Engineering Science Research Report, BLWT-3-69, University of Western Ontario, Canada, 1969.
[26] H. Tanaka, A.G. Davenport, Response of taut strip models to turbulent wind, *Journal of Engineering Mechanics Division ASCE* 108 (EM1) (1982) 33–49.
[27] P.A. Irwin, S.L. Gamble, Wind tunnel tests for the Annacis Island Bridge, Vancouver, British Columbia, Report No. 48515031 submitted to CBA Buckland and Taylor, Morrison Hershfield Ltd., 1985.
[28] S.J. Zan, The effect of mass, wind angle, and erection technique on the aeroelastic behaviour of a cable-stayed bridge model, Aeronautical Note, NAE-AN-46, NRC No. 28207, National Aeronautical Establishment, National Research Council Canada, Ottawa, Canada, 1987.
[29] G. Diana, M. Falco, S. Bruni, A. Cigada, G.L. Larose, A. Damsgaard, A. Collina, Comparison between wind tunnel tests on a full aeroelastic model of the proposed bridge over Stretto di Messina and numerical results, *Journal of Wind Engineering and Industrial Aerodynamics* 54/55 (1995) 101–113.
[30] T. Okubo, N. Narita, K. Yokoyama, H. Sato, Field observation of aerodynamic behavior of long-span bridges, *Proceedings of the Fifth International Conference on Wind Engineering,* Vol. 2, Fort Collins, Colorado, USA, 1979, pp. 825–839.
[31] J. Bietry, D. Delaunay, E. Conti, Comparison of full-scale measurement and computation of wind effects on a cable-stayed bridge, *Proceedings of Cable-stayed and Suspension Bridges,* Vol. 2, Deauville, 1994, pp. 109–116.
[32] L.D. Zhu, Y.L. Xu, F. Zhang, H.F. Xiang, Measurement of aerodynamic coefficients of tower components of Tsing Ma bridge under yaw winds, *Wind and Structures* 6 (1) (2003) 53–70.

[33] L.D. Zhu, Y.L. Xu, F. Zhang, H.F. Xiang, Tsing Ma bridge deck under skew winds—part I: aerodynamic coefficients, *Journal of Wind Engineering and Industrial Aerodynamics* 90 (2002) 781–805.
[34] L.D. Zhu, Y.L. Xu, H.F. Xiang, Tsing Ma bridge deck under skew winds—part II: flutter derivatives, *Journal of Wind Engineering and Industrial Aerodynamics* 90 (2002) 807–837.
[35] Z.H. Wang, Simulation of wind loading, *Journal of Building Structures* 15 (1) (1994) 44–52 (in Chinese).
[36] A. G. Davenport, The dependence of wind load upon meteorological parameters, *Proceedings of the International Research Seminar on Wind Effects on Buildings and Structures*, University of Toronto Press, Toronto, 1968, pp.19–82.
[37] J.B. Roberts, D. Surry, Coherence of grid-generated turbulence, *Journal of Engineering Mechanics Division ASCE* 99 (6) (1973) 1227–1245.
[38] E. Simiu, R.H. Scanlan, *Wind Effects on Structures: Fundamentals and Applications to Design*, third ed., Wiley, New York, USA, 1996.
[39] C. Dyrbye, S.O. Hansen, *Wind Loads on Structures*, Wiley, Chichester, England, UK, 1996.
[40] N.P. Jones, R. H. Scanlan, Advances (and challenges) in the prediction of long-span bridge response to wind, *Proceedings of International Symposium on Advances in Bridge Aerodynamics*, Copenhagen, Denmark, 1998, pp. 131–143.
[41] R.H. Scanlan, N.P. Jones, Aeroelastic analysis of cable-stayed bridges, *Journal of Structural Engineering ASCE* 11 (2) (1990) 279–297.
[42] R.W. Clough, J. Penzien, *Dynamics of Structures*, McGraw-Hill Inc., New York, USA, 1975.
[43] E.L. Wilson, A. Der Kiureghian, E.P. Bayo, A replacement for the SRSS method in seismic analysis, *Earthquake Engineering and Structural Dynamics* 9 (2) (1981) 187–192.
[44] J.H. Lin, A deterministic algorithm of stochastic seismic responses, *Journal of Earthquake Engineering and Vibration* 5 (1985) 89–94 (in Chinese).
[45] J.H. Lin, A fast CQC algorithm of PSD matrices for random seismic response, *Computer & Structures* 44 (3) (1992) 683–687.
[46] J.H. Lin, W.S. Zhang, J. Li, Structural responses to arbitrarily coherent stationary random excitations, *Computer & Structures* 50 (5) (1994) 629–633.
[47] D.E. Newland, *An Introduction to Random Vibrations, Spectral & Wavelet Analysis*, third ed., Longman Singapore Publishers Pte Ltd., Singapore, 1875.
[48] L.D. Zhu, Buffeting Response of Long Span Cable-supported Bridges under Skew Winds: Field Measurement and Analysis, PhD Dissertation, The Hong Kong Polytechnic University, Hong Kong, 2002.